SCMS SCHOOL OF ENGINEERING AND TECHNOLOGY,KARUKUTTY
BOOKS/CONFERENCE INDEX 2019-2020

3.3.2 Number of books and chapters in edited volumes/books published and papers published in national/ international conference proceedings per teacher during 2019-2020

Sl. No.	Name of the teacher	Title of the book/chapters published	Title of the paper	Title of the proceedings of the conference	Name of the conference	National / International	Calendar Year of publication	ISBN number of the proceeding	Affiliating Institute at the time of publication	Name of the publisher
1	Dr.Ratish Menon	A&WMA's 112th Annual Conference & Exhibition	Monitoring and analysis of gas emissions from a closed landfill site at Jleeb in Kuwait	A&WMA's 112th Annual Conference & Exhibition	A&WMA's 112th Annual Conference & Exhibition	International	Jun-19	ISBN: 978-1-5108-9682-6	SCMS Water Institute, SCMS School of Engineering and Technology,	Air & Waste Management Association
2	Dr.Ratish Menon	A&WMA's 112th Annual Conference & Exhibition	Study of the extent of contribution of regional stubble burning to the air pollution in Delhi-National Captial Region	A&WMA's 112th Annual Conference & Exhibition	A&WMA's 112th Annual Conference & Exhibition	International	Jun-19	ISBN: 978-1-5108-9682-7	SCMS School of Engineering and Technology, Ernakulam, India	Air & Waste Management Association
3	Remya Y K		Evaluation of current design practises for horizontal curves on rural highways bsead on vehicle stability and safety	NCIET- 2020 National Conference on Innovations in Engineering & Technology	International Journal of Innovative Research in Electrical, Electronics, Instrumentation and Control Engineering	International	Mar-20	ISSN (Print) 2278-1021, ISSN (Print) 2319-5940	SCMS School of Engineering and Technology, Ernakulam, India	IJIREEICE
4	Dr.Vidhya Chandran	Sustainable Development and Innovations in Marine Technologies	Controllability studies on fish-shaped unmanned under water vehicle undergoing manoeuvring motions			International	Aug-19	ISBN: 978036781008 5	SCMS School of Engineering and Technology, Ernakulam, India	CRC Press
5	Sindhya K Nambiar		POS Tagger for Malayalam using Hidden Markov Model	IEEE XPLORE	2019 International Conference on Smart Systems and Inventive Technology (ICSSIT)	International	Feb-20	978-1-7281-2120-8	SCMS School of Engineering and Technology, Ernakulam, India	IEEE

6	S Asha		Evasion Attacks On Svm Classifier	IEEE XPLORE	2019 9th International Conference on Advances in Computing and Communication (ICACC)	International	Feb-20	978-1-7281-5524-1	SCMS School of Engineering and Technology, Ernakulam, India	IEEE
7	Litty Koshy		RubiCrypt: Image Scrambling Encryption System Based on Rubik's Cube Configuration	IEEE XPLORE	2019 IEEE International Conference on System, Computation, Automation and Networking (ICSCAN)	International	Oct-19	978-1-7281-1525-2	SCMS School of Engineering and Technology, Ernakulam, India	IEEE
8	Dr.Varun G Menon	Data Management, Analytics and Innovation	Simulation based Performance Analysis of Location Based Opportunistic Routing Protocols in Underwater Sensor Networks (UWSN) having Communication Voids		Advances in Intelligent Systems and Computing book series (AISC,volume 1042)		Oct-19	978-981-32-9949-8	SCMS School of Engineering and Technology, Ernakulam, India	Springer Link
Total number of books and chapters in edited volumes/books published and papers published in national/ international conference proceedings per teacher during 2019-2020										**8**

SCMS SCHOOL OF ENGINEERING & TECHNOLOGY
KARUKUTTY
ERNAKULAM
683 576

PRINCIPAL
SCMS SCHOOL OF ENGINEERING & TECHNOLOGY
VIDYANAGAR, PALLISSERY, KARUKUTTY
ERNAKULAM, KERALA-683 576

https://link.springer.com/chapter/10.1007/978-981-32-9949-8_49

Simulation-Based Performance Analysis of Location-Based Opportunistic Routing Protocols in Underwater Sensor Networks Having Communication Voids

Conference paper | First Online: 25 October 2019

pp 697–711 | Cite this conference paper

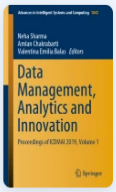

Data Management, Analytics and Innovation

https://link.springer.com/chapter/10.1007/978-981-32-9949-8_49

Check for updates

Cite this paper

John, S., Menon, V.G., Nayyar, A. (2020). Simulation-Based Performance Analysis of Location-Based Opportunistic Routing Protocols in Underwater Sensor Networks Having Communication Voids. In: Sharma, N., Chakrabarti, A., Balas, V. (eds) Data Management, Analytics and Innovation. Advances in Intelligent Systems and Computing, vol 1042. Springer, Singapore. https://doi.org/10.1007/978-981-32-9949-8_49

Download citation

.RIS .ENW .BIB

DOI
https://doi.org/10.1007/978-981-32-9949-8_49

Published
25 October 2019

Publisher Name
Springer, Singapore

Print ISBN
978-981-32-9948-1

Online ISBN
978-981-32-9949-8

eBook Packages
Engineering
Engineering (R0)

Simulation based Performance Analysis of Location Based Opportunistic Routing Protocols in Underwater Sensor Networks (UWSN) having Communication Voids

Sonali John[1], **Varun G Menon**[1] and **Anand Nayyar**[2]

[1]Department of Computer Science and Engineering,
SCMS School of Engineering and Technology, Kerala, India,
Email: varunmenon@scmsgroup.org

[2]Graduate School, Duy Tan University, Danang, Vietnam,
Email: anandnayyar@duytan.edu

Abstract

Recently, Underwater Wireless Sensor Networks (UWSNs) have emerged as a prominent research area in the networking domain due to its wide range of applications in submarine tracking, disaster detection, oceanographic data collection, pollution detection and underwater surveillance. With its unique characteristics like continuous movement of sensor nodes, limitations in bandwidth and high utilization of energy, efficient routing and data transfer in UWSNs have remained a challenging task for researchers. Almost all the protocols proposed for terrestrial sensor networks are inefficient and does not perform well in underwater environment. Recently location based opportunistic routing protocols have been observed to perform well in UWSN environments. But it is also observed that, these protocols suffer from performance degradation in UWSN networks with communication voids. The objective of this research paper is to discuss the working of major location based opportunistic routing protocols in UWSNs with communication voids and to highlight their related issues and drawbacks. We analyzed the Quality of Service (QoS) parameters, Packet Delivery Ratio (PDR), End-to-End delay, throughput and energy efficiency of two major location based opportunistic routing protocols i.e. Vector Based Forwarding (VBF) and Hop-by-Hop VBF (HH-VBF) in UWSNs with communication voids using NS-2 simulator with Aqua-Sim extension. Simulation results state that both VBF and HH-VBF protocols suffered from performance degradations in UWSNs with communication voids. In addition to this, the paper also highlights open issues for UWSN to assist researchers in designing efficient routing protocols for UWSNs having multiple communication voids.

Keywords: Communication void; Hop-by-Hop Vector-Based Forwarding (HH-VBF); Opportunistic Routing; performance analysis; Quality of Service (QoS); Underwater Wireless Sensor Networks (UWSNs); Vector-Based Forwarding (VBF); NS-2, AQUA-Sim.

Introduction

Recently, Underwater Wireless Sensor Networks (UWSNs) [1-2] have emerged as a prominent research area in the networking domain. The increasing interest in applying sensor networks into the underwater environment have found numerous applications in civilian and military fields such as coastline surveillance, pollution detection and underwater surveillance. In UWSNs, a group of sensors are placed at different depths in the ocean to gather information. This collected information is then forwarded to the target devices positioned at the surface via network of intermediate nodes. The data is then stored, processed and passed to different applications for appropriate utilization. As, radio signals have many limitations due to its mediocre propagation through water, acoustic medium is used between the sensor nodes in UWSNs [3]. Most of the applications are highly sensitive and their success relies on the accuracy of the collected data. Many recent applications of underwater sensor network ranging from aquaculture to the oil industry, instrument monitoring, climate recording, natural disturbances prediction and study of marine culture depends heavily on the accuracy of the collected data. Thus, efficient routing and data transfer among the nodes is vital in UWSNs.

Routing and data transfer from the sender to the sink stations, through the network, have been a tough task for researchers. Incessant movement of the nodes placed in the water due to the difference in the ocean environment and ocean currents is a major challenge. Limitations in bandwidth, frequent link interruptions, increased delay of data transfer, interference caused by marine mammals are some of the other elements influencing the efficiency of routing in UWSNs [4-5]. Due to these unique characteristics, almost all the protocols drafted for conventional sensor networks do not perform well in UWSNs [6]. Recently, Opportunistic Routing Protocols (ORPs) [7-9, 37] have found to give better performance in data transfer in UWSNs. The major advantage of this routing strategy is that it dynamically selects one best forwarder device from a group of candidate devices. This selection is based on the present scenario of the network, which leads to better performance of this latest category of protocols. Many ORPs have been designed for ad hoc, terrestrial sensor and UWSNs [10-14]. Amongst all categories in opportunistic routing, Location Based Opportunistic Routing Protocols (LBORPs) has found to give better performance. LBORPs make use of the knowledge on the present location of the devices to dynamically route message packets from the sender to target. Few location based ORPs have been efficiently used for data forwarding in UWSNs [15-21].

Communication holes or voids have been a major problem in most of the dynamic sensor networks. Often defined as the unreachability problem, the source node suffers from lack of adequate forwarder nodes in its transmission range. Frequent movement of sensor nodes in underwater increases this problem further. Limited research has been performed to determine the working and performance of LBORPs in UWSNs with communication voids [22-25]. In large UWSNs with limited number of sensors, it is very significant to have a protocol that can handle communication voids efficiently. In this article, we analyze the working and performance of two major LBORPs in UWSNs with communication holes. Vector Based Forwarding (VBF) [19] and Hop-by-Hop VBF (HH-VBF) [18, 26] have been used by many applications for data transfer in UWSNs. VBF is a LBORP that constructs a virtual vector pipe between the sender and sink node for routing. Only the devices within the virtual vector are selected for forwarding the data packet.

Extending VBF protocol, the HH-VBF protocol makes use of different virtual pipes for each node and the direction of the virtual pipe changes during the entire time of transmission.

Objectives of this research paper are,

- To study the functioning of major LBORPs designed for UWSNs and to determine their issues and drawbacks.
- To analyze the simulation-based performance comparison of VBF and HH-VBF protocols in UWSNs with communication voids on parameters- PDR, Throughput, End-to-End delay and energy efficiency.
- And, to discuss the issues, challenges and future directions in UWSNs routing research.

This research article is structured as follows. Functioning of the major location based ORPs in UWSNs is discussed in detail in section II. The section also discusses the issues and drawbacks with these protocols. Section III describes the working of VBF and HH-VBF in comprehensive manner. Section IV presents the simulation-based analysis of VBF and HH-VBF protocols in UWSNs having communication voids using NS2+Aqua-Sim simulator. Section V enlists open issues and challenges of existing ORPs in UWSNs. The paper concludes in section VI with future research directions.

II. Literature Survey

This section examines the functioning of some of the major LBORPs proposed for UWSNs. One of the most accepted protocol in UWSNs is Vector-Based Forwarding (VBF) [19]. VBF uses the details on the present position of the sensor devices for routing the information packets. In VBF, within a fixed virtual pipe the information packets are forwarded between the source and destination devices. These information packets are then transmitted along the redundant paths and thereby remain stable against packet loss. The major limitation with VBF is that the construction of a solitary virtual pipe will decrease the performance of routing in various node density areas and the productivity drops with communication holes.

Hop-by-Hop Vector-Based Forwarding (HH-VBF) [18] is a variant of the VBF protocol that uses virtual pipes from every intermediate device to the target device. Every device then dynamically make packet forwarding choices with reference to its present location in the network.

Directional Flood Based Routing (DFR) [29] is a receiver-based, stateless, and LBORP in which each and every node is informed about the position of the destination device and one-hop neighbors. DFR utilizes a limited flooding method, in which every node passes its location details to all the other nodes and achieves more reliability in data transmission in the network. The flooding mechanism results in duplicate transmissions and energy loss. DFR also failed to address the void problem.

One of the earliest protocols that functions with reference to the pressure information proposed for UWSNs was Depth-Based Routing (DBR) [30]. DBR utilizes the knowledge on the depth of devices placed underwater to decide whether to transmit the packets or not. When a packet is received, each node will forward the packet to a smaller depth than that stored in the packet. Otherwise, the packet is discarded. Both communication holes and node mobility are the major problems influencing the limited performance of DBR.

Geographic and opportunistic routing with Depth Adjustment-based topology control for communication Recovery over void regions (GEDAR) [31] is another location based anycast ORP that sends information packets from intermediate nodes to different target nodes. The protocol uses periodic beaconing to get the position information of every node in the network. The protocol suffers from increased duplicate message transmissions.

Hydraulic Pressure Based Anycast Routing (HydroCast) [32] also utilizes the knowledge on the depth of the deployed device to choose the candidates for routing from the nearest nodes. HydroCast elects a subgroup of neighboring devices with largest greedy progress to the target node. The performance of the protocol is not satisfactory with voids.

Multi-Path Routing (MPR) [33] helps to solve the data concussion issue at the sink nodes. The data collision is prevented at the receiving packets by creating a route that consists of various sub-paths between the sender and the sink. Geographic Partial Network Coding **(**GPNC) [35] is another geographic, partial network coding-based protocol proposed for UWSNs. Void is a major concern for this protocol too.

Focused Beam Routing (FBR) [34] was designed to minimize energy drainage during the routing process by controlled flooding of the packets. Although a preventive void handling technique was used, high delay was incurred.

Void-Aware Pressure Routing (VAPR) [35] uses an opportunistic data forwarding technique coupled with information on pressure of the deployed devices. VAPR select a subgroup of candidate devices with the greatest progress to target. The holding time details of two-hop neighboring nodes helps to deal with the void areas, but imposes a high overhead on the system.

In Relative Distance Based Forwarding (RDBF) [36], the packets are send via the nodes that are nearest to the target node. RDBF uses a fitness value as an upper limit to supervise the number of transmitting devices to the sink. Moreover, the performance of RDBF also comes down with the presence of communication holes in the network.

In the next two sections, we discuss the working of the two LBORPs, VBF and HH-VBF used in UWSNs. VBF and HH-VBF utilize the knowledge of the location of nodes in the network for routing. These protocols use greedy forwarding mechanism that chooses the node nearer to the target as the next forwarder for every data packet. We analyze the performances of these two protocols in UWSNs having multiple communication voids. We have selected these two protocols for the analysis because they are the two popular protocols used by various applications in UWSNs. Further the design of these protocols is less complex and also incurs less overhead compared to other protocols.

III. Location based Opportunistic Protocols

a) Vector-Based Forwarding (VBF)

VBF [19, 38] was proposed to addresses the problem of energy limitation and efficient packet delivery. VBF utilize the knowledge of the location of nodes in the network for routing. Each data packet in VBF contains the three position fields named as OP1, TP1 and FP1. This represents the coordinates of the source, the sink and the forwarder node. The RANGE field in the packet deals with node mobility. As soon as the information packet advances to the region marked by its TPI, it is flooded in that region controlled by RANGE field. The virtual routing vector from the source to the sink describes the transmitting path. The RADIUS field inside the

packet is a pre-computed value that is utilized by intermediate devices to check whether they are near to the vector pipe and suitable for packet transmission. In order to limit the number of intermediate transmitting devices and to conserve energy in the network, VBF make use of a self-adaptive algorithm. Upon getting a data packet, each node first computes whether it is inside the virtual vector, and whether it can act as a potential forwarder to the next node. Each potential member device awaits a limited period of time to check its desirability value in the pipe. It describes the closeness of the current node to the past forwarder node, and the virtual pipe between sender and sink. The waiting time depends on the desirability factor. If a node is more desirable, then it waits less time. During this time, the device pays attention to the channel to observe the number of devices that are transmitting the same information packet as the present device. When the period expires, the node will transmit its packet, if and only if the reduced desirability value of the other nodes is less than a pre-computed level.

Virtual routing pipe in VBF is illustrated in figure 1. We can see that VBF has created three independent virtual pipes from source nodes S1, S2 and S3 to the destination D at the surface. In figure 1, S1, D represents the source and target node. Only the devices within the vector pipe are considered for forwarding a packet, thereby limiting the energy usage.

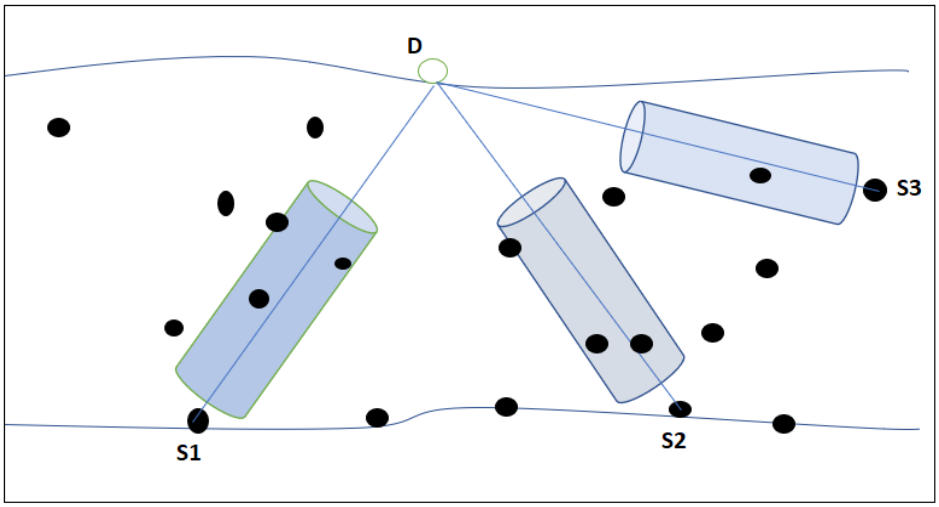

Figure 1. Virtual vector pipe from sender to receiver node in VBF

b) **Hop-by-Hop Vector-Based Forwarding (HH-VBF)**

Hop-By-Hop Vector-Based Forwarding (HH-VBF) [18] is a variant of VBF that constructs virtual routing pipes from each hop in the network, as packets travel from the sender device to the receiver. This protocol creates a virtual routing pipe from each hop to the target device. Many studies have discussed the better working of HH-VBF in comparison with VBF. The pipeline radius is similar as the transmission count of the node. The protocol improves the direction of the transmitting pipe hop by hop, in the entire life period and in this way, all transmitting devices can generate a routing choice based on the present local topology details. By changing the direction of flooding pipeline dynamically, the performance can be enhanced. When a stable routing vector radius is set, the protocol shows a reduced performance in the

sparse network compared with VBF. However, both the protocols are exposed to interferences caused by marine mammals as the data forwarding happens only inside the pipe. Here the transmission can be interrupted when marine mammals block the pipe. There is an increased choice of finding a more acceptable forwarder within the hop-by-hop vector pipeline; HH-VBF gives better Packet Delivery Ratio (PDR). However, both the protocols does not succeed to yield energy fairness within the network. Also fails to effectively handle the communication hole problem.

The working of HH-VBF is described in figure 2. The sender node S2 wants to transmit an information packet to the destination device D2. Here S2 creates a virtual pipe to the destination D2. Once the packet reaches the intermediate sensor node M, it creates a virtual pipe to the destination. Now there are more nodes (N and P) included for sending the data packet to the target location. HH-VBF uses this forwarding strategy till the data reaches the target location. HH-VBF improves the performance in the network by dynamically moving the direction of flooding pipe. Figure 3 illustrates the communication void problem in UWSNs. We can see that source node S1 and S2 are trying to forward data packets to the destination D by creating virtual pipes. Data from S2 reaches the destination node located at the surface, but data from source S1 is unable to proceed due to the communication void near to the surface. Table 1 highlights the technical comparison of both the routing protocols.

Table 1. Comparison of VBF and HH-VBF

Parameter	**VBF**	**HHVBF**
Metric used	Node location	Node Location
Candidate Coordination	Timer based	Timer based
Void Handling	No	No
Routing	Single Virtual Pipe from the sender to the destination	Individual virtual pipes from each transmitting device to target device
Advantages	Simple and flexible	Simple and flexible
Limitations	Duplicate messages and transmissions Performance degrades with communication holes	Performance degrades with communication holes

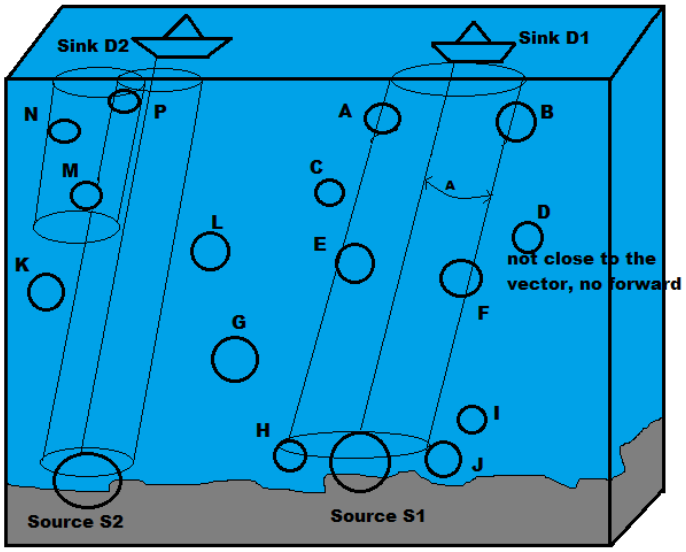

Figure 2. Illustration of the functioning of VBF and HH-VBF

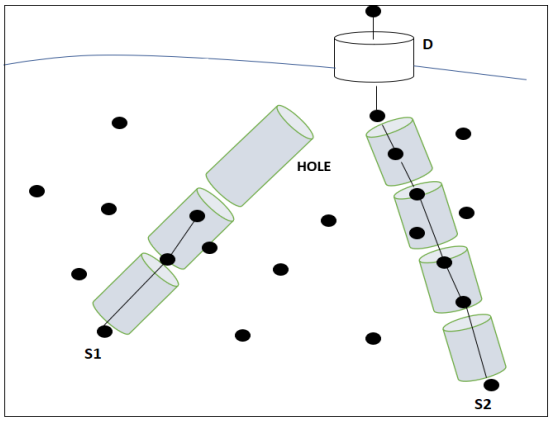

Figure 3. Communication void problem with VBF

IV. Simulation and Performance Analysis

a. Simulation Parameters

Performance of VBF and HH-VBF routing protocols are analyzed using simulations in Aqua-Sim[39]. Aqua-Sim is extended version of NS-2 that efficiently simulates collision behaviors in large delay acoustic networks and also attenuation of underwater sensor networks. Aqua-Sim uses otcl to model the protocol parameters implemented through C++ algorithms. The simulator creates a 3D environment of packet transmission in the network, which shows that the efficiency of both protocols comes down with communication holes. Communication voids are created between the source and sink devices to measure QoS parameters in the overall network.

Table 2 highlights the Simulation Parameters used to test the performance of the protocols in Aqua-Sim

Table 2. Simulation Parameters

Parameter name	Values
Simulator name	NS2.35 + Aqua-sim
Dimension of topology	1500 x 1500 x 1500 m
Transmission range	250 m
Antenna-Type	Omn-Directional
Data rate	50 kbps
Packet size	25 to 125 bytes
Number of nodes	100 to 600
Simulation time	300 s
Number of Simulation runs	10
Protocols	VBF, HH-VBF

b. Performance Analysis

The performances of VBF and HH-VBF protocols were analyzed in normal network scenario and in networks with communication void. Figure 4 shows the values of various parameters used in simulations. Four different QoS parameters were measured in the network.

- **Packet Delivery Ratio (PDR):** PDR is the ratio of overall packets arrived at the target device to the number of transmitted packets.

The following Figure 4 shows the PDR in UWSN network scenario with varying number of nodes for the two protocols in normal network conditions and also with communication voids. Table 3 highlights the data values of VBF, VBF-VOID, HH-VBF and HH-VBF void. From the analysis it is observed that both VBF and HH-VBF protocols give better performances in networks without communication voids. This proves that communication voids degrade the performance of even the latest LBORPs in UWSNs.

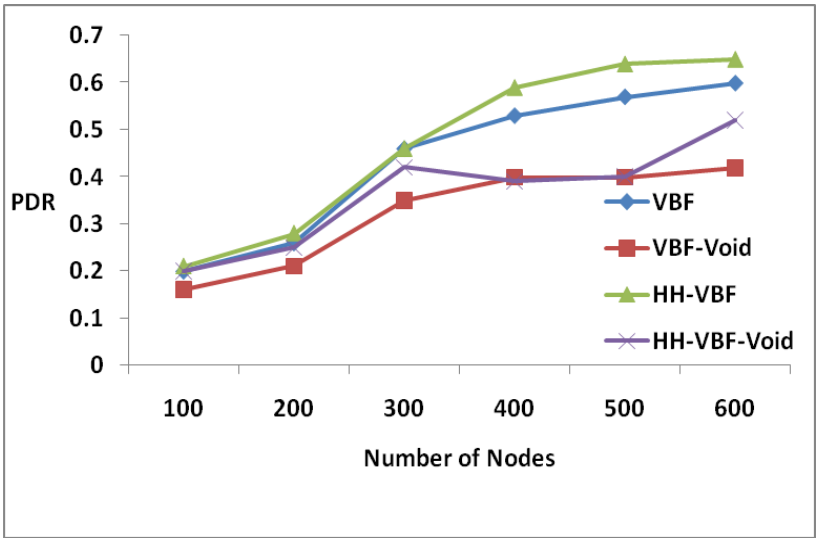

Figure 4. PDR vs Nodes

Table 3: PDR

No. of Nodes	VBF	VBF-Void	HH-VBF	HH-VBF-Void
100	0.2	0.16	0.21	0.2
200	0.26	0.21	0.28	0.25
300	0.46	0.35	0.46	0.42
400	0.53	0.4	0.59	0.39
500	0.57	0.4	0.64	0.4
600	0.599	0.42	0.65	0.52

.

- **Average End to End Delay:** It is the time incurred by the information packet in reaching the target device from the sender device.

Figure 5 highlights the average delay incurred by VBF, HH-VBF protocols in transferring data packets across the network with varying number of devices in normal and void environments. Table 4 highlights the data analysis of delay observed by routing protocols with void and under normal operating conditions. From the data values, it is evident that the delay is less VBF and HH-VBF in normal environments as compared to networks with voids.

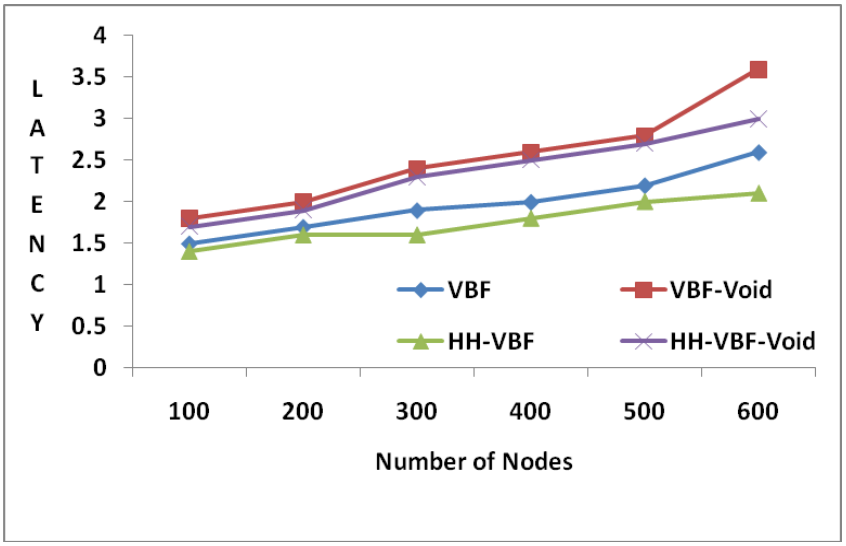

Figure 5. Latency/End-To-End Delay vs Nodes

Table 4: Average end to end delay

No. of nodes	VBF	VBF-Void	HH-VBF	HH-VBF-Void
100	1.5	1.8	1.4	1.7
200	1.7	2	1.6	1.9
300	1.9	2.4	1.6	2.3
400	2	2.6	1.8	2.5
500	2.2	2.8	2	2.7
600	2.6	3.6	2.1	3

- **Throughput:** It is the rate or amount of data that is effectively transferred from the sender device to the target in a given time period.

Figure 6 highlights the throughput of both VBF and HH-VBF protocols in normal and void environments. Table 5 enlists the data values of throughput. It is observed that HH-VBF protocol has highest throughput as compared to other routing protocols. Both the protocol suffer from degradation in throughput with voids in the network.

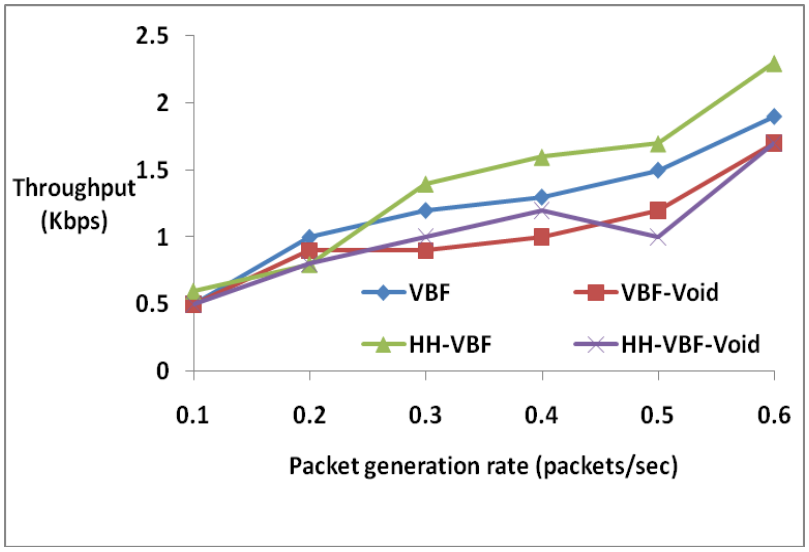

Figure 6. Throughput vs packet generation rate

Table 5: Throughput

Packet generation rate	VBF	VBF-Void	HH-VBF	HH-VBF-Void
0.1	0.5	0.5	0.6	0.5
0.2	1	0.9	0.8	0.8
0.3	1.2	0.9	1.4	1
0.4	1.3	1	1.6	1.2
0.5	1.5	1.2	1.7	1
0.6	1.9	1.7	2.3	1.7

- **Energy Consumption:** In order to test the validity of performance of routing protocols, Energy consumption is regarded as significant parameter. Energy Consumption is regarded as how much energy is consumed by transmitting nodes and intermediary nodes to make sure that packet reaches the destination.

Figure 7 elaborates the graphical analysis of energy consumption of energy nodes in different protocols under UWSN operating scenarios. Table 6 also highlights the data values of protocols and it is observed that both protocols consume more energy in void scenarios.

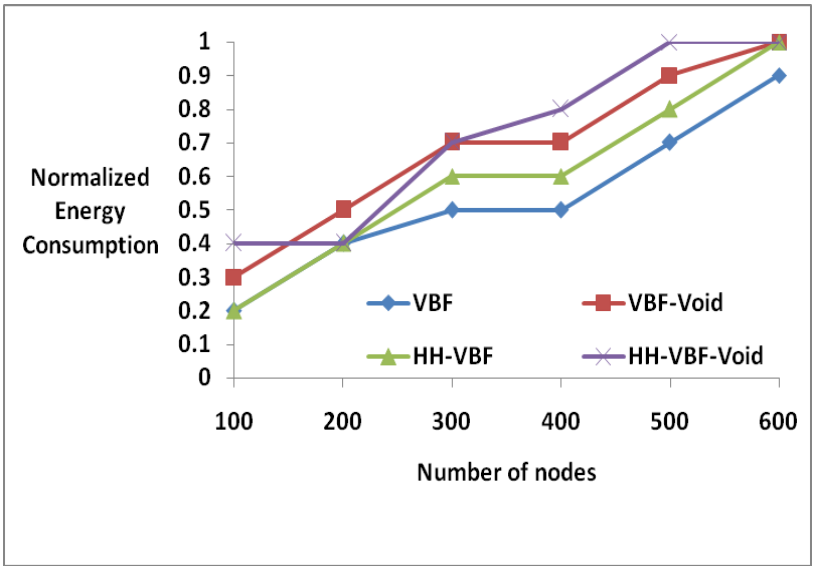

Figure 7. Normalized Energy Consumption vs No. of nodes

Table 6: Normalized Energy Consumption

No. of nodes	VBF	VBF-Void	HH-VBF	HH-VBF-Void
100	0.2	0.3	0.2	0.4
200	0.4	0.5	0.4	0.4
300	0.5	0.7	0.6	0.7
400	0.5	0.7	0.6	0.8
500	0.7	0.9	0.8	1
600	0.9	1	1	1

V. Open Research Areas and Recommendations

In this section, open research problems generated by communications holes in UWSNs are discussed. Researchers designing routing protocols need to address the following issues to come up with optimal routing solutions for UWSN scenarios.

- Quality of Service (QoS): Communication voids drastically degrade the QoS offered by the routing protocols in UWSNs. The data delivery rate is reduced with increased data loss due to communication holes and void nodes. Delay in data transmission increases

with frequent loss of data packets.

- Reliability: Reliable data delivery is a vital factor in the success of any routing protocol. Void nodes are often unable to find the next forwarder node in the network and are forced to drop the data packet. Thus, reliability is a big concern in UWSNs with communication voids.
- Scalability: In many UWSNs, the problems of communication holes occur when the network size is increased. With reduced number of sensor nodes in large geographical area, the chances are high for the occurrence of communication holes. Solutions to avoid communication voids with minimum number of sensor node are to be found out.
- Mobility: Frequent mobility of sensor nodes is another reason for the communication voids. Good protocols should handle mobility of nodes effectively for better performance.
- Energy: Loss of energy due to communication voids is another area of concern. With constrained battery, and inability in frequent recharges, underwater sensor nodes need to be protected from unwanted drainage of energy.

VI. Conclusion and Future Work

Underwater Sensor Networks have come out as a prominent research area in the networking domain with a wide range of aquatic applications. Routing in UWSNs is an area of major concern due to its unique features such as continuous node mobility, frequent disruption of links, and interference caused by other underwater acoustic systems such as marine mammals. Recently in UWSNs, opportunistic routing has been accepted as an efficient routing approach. The paper discussed the functioning of various location based opportunistic routing protocols proposed for UWSNs and evaluated the performance of two major protocols, VBF and HH-VBF using simulations in Aqua-Sim. The performances of these protocols are evaluated in normal network scenarios and also in networks with communication voids. We could observe that the performance of these protocols comes down with communication voids in the network. Insights from this article would enable researchers to work towards designing more effective protocols for underwater environments having voids. In the near future, a novel routing protocol, especially designed for UWSN operating scenarios would be proposed and compared with existing routing protocols in terms of PDR, Energy, Delay and Throughput and above all will give good performance in networks with communication voids and highly secure from all sorts of intruder and man-in-middle attack.

References

[1] Sozer, E., Stojanovic, M., & Proakis, J. (2000). Underwater acoustic networks. *IEEE Journal of Oceanic Engineering*, *25*(1), 72-83. doi:10.1109/48.820738

[2] Jun-Hong Cui, Jiejun Kong, Gerla, M., & Shengli Zhou. (2006). The challenges of building scalable mobile underwater wireless sensor networks for aquatic applications. *IEEE Network*, *20*(3), 12-18. doi:10.1109/mnet.2006.1637927.

[3] Akyildiz, I. F., Pompili, D., & Melodia, T. (2005). Underwater acoustic sensor networks: research challenges. *Ad Hoc Networks*, *3*(3), 257-279. doi:10.1016/j.adhoc.2005.01.004.

[4] Akyildiz, I. F., Pompili, D., & Melodia, T. (2006). State-of-the-art in protocol research for underwater acoustic sensor networks. *Proceedings of the 1st ACM international workshop on Underwater networks - WUWNet '06*. doi:10.1145/1161039.1161043

[5] Açar, G., & Adams, A. (2006). ACMENet: an underwater acoustic sensor network protocol for real-time environmental monitoring in coastal areas. *IEE Proceedings - Radar, Sonar and Navigation*, *153*(4), 365. doi:10.1049/ip-rsn:20045060.

[6] Partan, J., Kurose, J., & Levine, B. N. (2006). A survey of practical issues in underwater networks. *Proceedings of the 1st ACM international workshop on Underwater networks - WUWNet '06*. doi:10.1145/1161039.1161045

[7] Biswas, S., & Morris, R. (2005). ExOR. *ACM SIGCOMM Computer Communication Review*, *35*(4), 133. doi:10.1145/1090191.1080108

[8] Bruno, R., Conti, M., & Nurchis, M. (2010). Opportunistic packet scheduling and routing in wireless mesh networks. *2010 IFIP Wireless Days*. doi:10.1109/wd.2010.5657736

[9] Chakchouk, N. (2015). A Survey on Opportunistic Routing in Wireless Communication Networks. *IEEE Communications Surveys & Tutorials*, *17*(4), 2214-2241. doi:10.1109/comst.2015.2411335

[10] Menon, V. G., & Prathap, P. M. (2016). Comparative analysis of opportunistic routing protocols for underwater acoustic sensor networks. *2016 International Conference on Emerging Technological Trends (ICETT)*. doi:10.1109/icett.2016.7873733

[11] Menon V G, (2018). Opportunistic Routing Protocols in Underwater Acoustic Sensor Networks: Issues, Challenges, and Future Directions. *Magnetic Communications: From Theory to Practice*, CRC Press, pp. 127-148.

[12] Menon, V. G., & Prathap, P. M. (2017). Moving From Topology-Dependent to Opportunistic Routing Protocols in Dynamic Wireless Ad Hoc Networks: Challenges and Future Directions. *Algorithms, Methods, and Applications in Mobile Computing and Communications*, IGI Global, pp.1-23.

[13] Menon V G, (2017). Analyzing the Performance of Random Mobility Models with Opportunistic Routing" *Advances in Wireless and Mobile Communications*, 10(5), pp. 1221-1226.

[14] Han, M. K., Bhartia, A., Qiu, L., & Rozner, E. (2011). O3. *Proceedings of the Twelfth ACM International Symposium on Mobile Ad Hoc Networking and Computing - MobiHoc '11*. doi:10.1145/2107502.2107505

[15] Ayaz, M., Abdullah, A., Faye, I., & Batira, Y. (2012). An efficient Dynamic Addressing based routing protocol for Underwater Wireless Sensor Networks. *Computer Communications*, *35*(4), 475-486. doi:10.1016/j.comcom.2011.11.014

[16] Yan, H., Shi, Z. J., & Cui, J. (2008). DBR: Depth-Based Routing for Underwater Sensor Networks. *NETWORKING 2008 Ad Hoc and Sensor Networks, Wireless Networks, Next Generation Internet*, 72-86. doi:10.1007/978-3-540-79549-0_7

[17] Jafri, M. R., Sandhu, M. M., Latif, K., Khan, Z. A., Yasar, A. U., & Javaid, N. (2014). Towards Delay-sensitive Routing in Underwater Wireless Sensor Networks. *Procedia Computer Science*, *37*, 228-235. doi:10.1016/j.procs.2014.08.034

[18] Chen Wang, Gang Zhang, Lei Zhang, & Yang Shao. (2015). Improvement research of underwater sensor network routing protocol HHVBF. *11th International Conference on Wireless Communications, Networking and Mobile Computing (WiCOM 2015)*. doi:10.1049/cp.2015.0744

[19] Xie, P., Cui, J., & Lao, L. (2006). VBF: Vector-Based Forwarding Protocol for Underwater Sensor Networks. *NETWORKING 2006. Networking Technologies, Services, and Protocols; Performance of Computer and Communication Networks; Mobile and Wireless Communications Systems*, 1216-1221. doi:10.1007/11753810_111

[20] Ghoreyshi, S., Shahrabi, A., & Boutaleb, T. (2016). A Novel Cooperative Opportunistic Routing Scheme for Underwater Sensor Networks. *Sensors*, *16*(3), 297. doi:10.3390/s16030297

[21] Nicolaou, N., See, A., Xie, P., Cui, J., & Maggiorini, D. (2007). Improving the Robustness of Location-Based Routing for Underwater Sensor Networks. *OCEANS 2007 - Europe*. doi:10.1109/oceanse.2007.4302470

[22] Ghoreyshi, S. M., Shahrabi, A., & Boutaleb, T. (2017). Void-Handling Techniques for Routing Protocols in Underwater Sensor Networks: Survey and Challenges. *IEEE Communications Surveys & Tutorials*, *19*(2), 800-827. doi:10.1109/comst.2017.2657881

[23] Menon, V. G., & Joe Prathap, P. M. (2015). Opportunistic Routing with Virtual Coordinates to Handle Communication Voids in Mobile Ad hoc Networks. *Advances in Intelligent Systems and Computing*, 323-334. doi:10.1007/978-3-319-28658-7_28

[24] Ghoreyshi, S. M., Shahrabi, A., & Boutaleb, T. (2016). An Opportunistic Void Avoidance Routing Protocol for Underwater Sensor Networks. *2016 IEEE 30th International Conference on Advanced Information Networking and Applications (AINA)*. doi:10.1109/aina.2016.96

[25] Menon, V. G., & Prathap, P. M. (2017). A Review on Efficient Opportunistic Forwarding Techniques used to Handle Communication Voids in Underwater Wireless Sensor Networks, *Advances in Wireless and Mobile Communications*, 10(5), pp. 1059-1066.

[26] Darehshoorzadeh A., & Boukerche, A. (2015) Underwater Sensor Networks: A New Challenge for Opportunistic Routing Protocols. *IEEE Communications Magazine*. 53(11), pp. 98-107,

[27] P. Xie et al. (2009). Aqua-Sim: An NS-2 based simulator for underwater sensor networks. *OCEANS 2009*, Biloxi, MS, 2009, pp. 1-7.

[28] Martin, R., Zhu, Y., Pu, L., Dou, F., Peng, Z., Cui, J., & Rajasekaran, S. (2015). Aqua-Sim Next Generation. *Proceedings of the 10th International Conference on Underwater Networks & Systems - WUWNET '15*. doi:10.1145/2831296.2831341

[29] Daeyoup Hwang, & Dongkyun Kim. (2008). DFR: Directional flooding-based routing protocol for underwater sensor networks. *OCEANS 2008*. doi:10.1109/oceans.2008.5151939

[30] Yan, H., Shi, Z. J., & Cui, J. (2008). DBR: Depth-Based Routing for Underwater Sensor Networks. *NETWORKING 2008 Ad Hoc and Sensor Networks, Wireless Networks, Next Generation Internet*, 72-86. doi:10.1007/978-3-540-79549-0_7

[31] Coutinho, R. W., Boukerche, A., Vieira, L. F., & Loureiro, A. A. (2014). GEDAR: Geographic and opportunistic routing protocol with Depth Adjustment for mobile underwater sensor networks. *2014 IEEE International Conference on Communications (ICC)*. doi:10.1109/icc.2014.6883327

[32] Chen, Y.S., Juang, T.Y., Lin, Y.W. & Tsai, I.C. (2010). A Low Propagation Delay Multi-Path Routing Protocol for Underwater Sensor Networks. *J. Internet Technol*. 11, 153–165.

[33] Hao, K., Jin, Z., Shen, H., & Wang, Y. (2015). An Efficient and Reliable Geographic Routing Protocol Based on Partial Network Coding for Underwater Sensor Networks. *Sensors*, *15*(6), 12720-12735. doi:10.3390/s150612720

[34] Jornet, J. M., Stojanovic, M., & Zorzi, M. (2008). Focused beam routing protocol for underwater acoustic networks. *Proceedings of the third ACM international workshop on Wireless network testbeds, experimental evaluation and characterization - WuWNeT '08*. doi:10.1145/1410107.1410121

[35] Noh, Y., Lee, U., Wang, P., Choi, B. S., & Gerla, M. (2013). VAPR: Void-Aware Pressure Routing for Underwater Sensor Networks. *IEEE Transactions on Mobile Computing*, *12*(5), 895-908. doi:10.1109/tmc.2012.53

[36] Li, Z. L., Yao, N. M., & Gao, Q. (2013). Relative Distance-Based Forwarding Protocol for Underwater Wireless Sensor Networks. *Applied Mechanics and Materials*, *437*, 655-658. doi:10.4028/www.scientific.net/amm.437.655

[37] Nayyar, A., Batth, R. S., Ha, D. B., & Sussendran, G. (2018). Opportunistic Networks: Present Scenario-A Mirror Review. *International Journal of Communication Networks and Information Security (IJCNIS)*, *10*(1).

[38] Nayyar, A., Puri, V., & Le, D. N. (2019). Comprehensive Analysis of Routing Protocols Surrounding Underwater Sensor Networks (UWSNs). In *Data Management, Analytics and Innovation* (pp. 435-450). Springer, Singapore.

[39] Nayyar, A., & Singh, R. (2015). A comprehensive review of simulation tools for wireless sensor networks (WSNs). *Journal of Wireless Networking and Communications*, *5*(1), 19-47.

RubiCrypt: Image Scrambling Encryption System Based on Rubik's Cube Configuration

Publisher: IEEE

Joffin Joy ; Litty Koshy **All Authors** •••

Abstract: This paper proposes an image-encryption algorithm based on the Rubik's cube configuration,allowing for multi-dimensional security keys. The input image is scrambled using... **View more**

Metadata

Abstract:
This paper proposes an image-encryption algorithm based on the Rubik's cube configuration,allowing for multi-dimensional security keys. The input image is scrambled using the random configuration of a Rubik's cube. Here the aim is to encrypt or decrypt an image using a custom pixel scrambling algorithm. It uses a Rubik's Cube as the encryption & decryption key, which allows for 43,252,003,274,489,856,000 (43 quintillion) distinct key configurations. RubiCrypt makes use of several image processing algorithms from OpenCV for scanning the cube in real-time. Finally, Analysis along with experimental results shows that the proposed encryption scheme can achieve good encryption as well asconsiderable hide-ability. Which can resist all the elements related with statistical and differential attacks.

Published in: 2019 IEEE International Conference on System, Computation, Automation and Networking (ICSCAN)

Date of Conference: 29-30 March 2019

INSPEC Accession Number: 19082869

Date Added to IEEE *Xplore*: 24 October 2019

DOI: 10.1109/ICSCAN.2019.8878785

▸ ISBN Information:

Publisher: IEEE

Conference Location: Pondicherry, India

Contents

Privacy is one of the key factors governing a technological deployment. The end user privacy is always kept in mind by developers all over the world. Especially in areas such as cloud computing which holds large contents of digital user data, mere raw input to these systems makes the user data unsafe.

EVASION ATTACKS ON SVM CLASSIFIER

Maria
Computer Science and Engineering Dept
SCMS School of Engineering and Technology
Ernakulam, India
mariatoffee97@gmail.com

Mikhiya James
Computer Science and Engineering Dept
SCMS School of Engineering and Technology
Ernakulam, India
mikhiyajames@gmail.com

Mruthula M
Computer Science and Engineering Dept
SCMS School of Engineering and Technology
Ernakulam, India
mruthula.m.manmadhan@gmail.com

Vismaya Bhaskaran
Computer Science and Engineering Dept
SCMS School of Engineering and Technology
Ernakulam, India
vismayabhaskaran97@gmail.com

Asha S
Computer Science Dept
SCMS School of Engineering and Technology
Ernakulam, India
ashas@scmsgroup.org

***Abstract*— Support Vector Machine (SVM) is one of the main classification techniques used in many security-related applications like malware detection, spam filtering, etc. To incorporate SVM into real-world security applications they must be able to cope up with the attack patterns that will lead to misclassifications. In this system, the vulnerability of SVM to evasion attacks are measured. A simple but effective approach is presented that can be exploited to systematically assess the security of widely-used classification algorithms against evasion attacks. To identify the vulnerabilities some transformations are applied to the testing set of handwritten digit images. The obtained result is plotted as a confusion matrix that allows the visualization of the performance of the algorithm against evasion attack. The work demonstrates the correctness and performance of existing adversarial systems. This work also compares the performance level of feature descriptors like Speeded Up Robust Features (SURF) and Histogram of Oriented Gradients (HOG) and their level of vulnerability to the evasion attacks are also measured. It can be inferred from our system that, even though both HOG and SURF are vulnerable to evasion attacks, those images that are extracted using SURF is less vulnerable compared to those images extracted using HOG features.**

***Keywords*— HOG, SURF, Evasion Attacks, SVM**

I. INTRODUCTION

Nowadays machine learning algorithms are used in a wide range of applications. It is widely used in security sensitive applications such as malware detection and spam detection because of its ability to detect attacks or variants of known ones. Evasion attacks [6] are the most popular type of attack that can occur during system operation in adversarial settings. Evasion attacks manipulate the input data at test time and cause misclassifications. Even though many pattern recognition techniques are used in security sensitive applications to distinguish between malicious and legitimate samples, still there exist some attackers who intent to misclassify malicious data as legitimate data at test time. Current research shows the fact that SVM are vulnerable to evasion attacks as they never consider the existence of an attack. Adversarial machine learning algorithms [7] are built to exploit the vulnerabilities in a machine learning algorithm. These vulnerabilities are simulated by training the learning algorithm under various attack scenarios and policies. To better understand the vulnerability of SVM classifier in adversarial settings some manipulations are made in the input data at test time.

The main objective of the work is to identify the vulnerabilities in SVM classifier to evasion attacks. The success of a machine learning algorithm depends on their resistance to adversarial data. To identify the vulnerabilities some transformations are applied on the testing set of handwritten digit images. The number of correct and incorrect predictions is summarised by plotting a confusion matrix. Our system also compares the performance level of feature descriptors like SURF and HOG and their level of vulnerability to the evasion attacks are also measured.

II. RELATED WORKS

Support Vector Machine [3] is one of the most commonly used classification technique. In [2], it is observed that SVM trained on HOG feature vector identified objects similar to a human visual system. In [1], HOG (Histogram of Oriented Gradients) which are locally normalised show excellent performance compared to other existing feature set for human detection in images. Lowe in [4] showed that feature extracted using local interest points detects objects more efficiently than global feature vectors. Bay, Herbert et.al in [5] introduced an effective local feature descriptor SURF (Speeded Up Robust Features). SURF being invariant to transformation can correctly classify objects subjected to transformation attacks. In [8], the systems portraits the various image transformations that can be applied to images in order to cause an adversarial effect.

978-1-7281-5523-4/19/$31.00 ©2019 IEEE

III. METHODOLOGY

The basic architecture of our system is depicted in Figure. 1. Here, numerical digits features are extracted using HOG (Histogram of Oriented Gradient) and SURF (Speeded Up Robust Features) and classified using a multi-class SVM classifier. In this work, using the features extracted from the training set, the SVM classifier is trained. The basic procedure for creating an object classifier is:

- Acquire a labelled data set.
- The data set is partitioned into a training set and a test set.
- Train the classifier using features extracted from the training set.
- Test the classifier using features extracted from the test set.

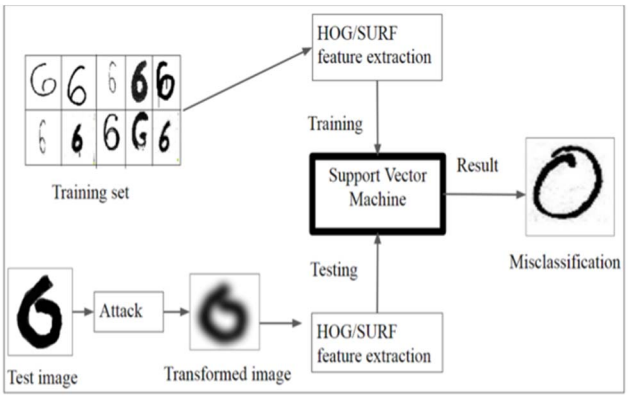

Figure 1. Architecture Diagram

A. Training Dataset Generation

For training, digit images taken from the MNIST database (Modified National Institute of Standards and Technology database) .Each image in the training set is surrounded by other digits, this is to recreate the real world scenario.

B. Test Dataset Generation

For testing, handwritten images of digits are used. These handwritten digits are taken from the MNIST database .MNIST is a large database of handwritten digits which are normally used for training and testing.

C. Feature Extraction

a) HOG Features: HOG stands for Histogram of Oriented Gradients. HOG is a feature descriptor where the histogram of directions of gradients are used as features. HOG [1] [2] feature vectors extracted from the training images are the data used to train the classifier. It is therefore important to ensure that the proper amount of information about the object is encoded by the HOG feature vector. Gradients of an image are useful because the magnitude of gradients is large around edge corners and edges pack a lot of information about object shape. For HOG feature extraction, first calculate the horizontal and vertical gradients and then calculate the histogram of gradients. Finally the histograms are combined into one giant vector.

b) SURF Features: SURF stands for Speeded Up Robust Features. SURF is a local feature detector and a feature descriptor that relies on local haar wavelet responses. SURF is a speeded-up version of Scale - Invariant Feature Transformation (SIFT).SURF (Speeded Up Robust Features) [5] is a kind of feature extractor and also a matcher for the points of interest in any image and the extracted features used in object recognition. SURF feature extraction is based on the same methodology as well as stages as that of SIFT. SURF is implemented either by approximating LoG(Laplacian of Gaussian) with Box Filter for finding scale-space or by relying on determinant of the Hessian matrix for both scale and location.

D. Training

Digit classification is a multiclass classification problem, where an image is classified into one out of the ten possible digit classes 0-9. During training phase, the extracted HOG features from the training set are used to train the classifier. Multiclass linear SVM is used as the classifier.

E. Attack Generation

Transformations such as gamma correction, blur, sharpen, rotation etc. are applied on the handwritten digit images to validate how the classifier performed on data. These transformations allow a small, carefully designed change to input and thus completely alter the output of the system.

a) Blur: The shape of an object is due to its edges, so in blurring we simply reduce the edge content and makes the transition from one colour to other smooth. Filter used for blurring is normally a low pass filter, because it allows low frequency and stop high frequency. Around edge pixel value (frequency) changes rapidly, as a result high frequency will be filtered out.

b) Gamma Correction : Gamma correction control the overall brightness of an image. Varying the amount of gamma correction not only changes the brightness of an image but also changes the ratio of red to green to blue.

c) Sharpen: Sharpening is opposite to blur. Blurring is performed by reducing the edge content and sharpening is performed by increasing the edge content. For these, edges are found by any of operator and it is added to the image. And thus image would have more edges, and it looks like sharpen.

d) Rotation : Image rotation is performed in order to rotate the image at any desired angle. And here, image is rotated only at small degree to avoid a major change in the appearance of the image.

F. Testing

Evaluate the digit classifier using images from the test set after applying the transformations. The evaluation returns the confusion matrix, which is a good initial indicator of how well the classifier is performing. As in the training step, HOG features and SURF features are extracted from the test images. These features will be used to make the final predictions

digit	0	1	2	3	4	5	6	7	8	9
0	0.25	0.00	0.08	0.00	0.00	0.00	0.67	0.00	0.00	0.00
1	0.00	0.42	0.00	0.08	0.08	0.00	0.00	0.25	0.08	0.08
2	0.00	0.00	0.75	0.17	0.00	0.00	0.00	0.00	0.00	0.08
3	0.00	0.00	0.00	0.67	0.00	0.00	0.17	0.00	0.17	0.00
4	0.00	0.00	0.00	0.25	0.75	0.00	0.00	0.00	0.00	0.00
5	0.00	0.00	0.00	0.00	0.00	0.33	0.67	0.00	0.00	0.00
6	0.00	0.00	0.08	0.00	0.50	0.00	0.42	0.00	0.00	0.00
7	0.00	0.00	0.25	0.42	0.00	0.00	0.00	0.25	0.08	0.00
8	0.00	0.00	0.17	0.08	0.00	0.00	0.00	0.00	0.75	0.00
9	0.00	0.08	0.00	0.17	0.08	0.08	0.00	0.00	0.25	0.33

Figure 2. HOG: Before Transformation

digit	0	1	2	3	4	5	6	7	8	9
0	0.17	0.00	0.08	0.00	0.00	0.00	0.67	0.00	0.08	0.00
1	0.00	0.50	0.00	0.17	0.08	0.00	0.00	0.17	0.08	0.00
2	0.00	0.00	0.67	0.17	0.00	0.00	0.08	0.00	0.08	0.00
3	0.00	0.00	0.00	0.67	0.00	0.00	0.17	0.00	0.17	0.00
4	0.00	0.00	0.00	0.25	0.75	0.00	0.00	0.00	0.00	0.00
5	0.00	0.00	0.00	0.00	0.00	0.42	0.50	0.00	0.08	0.00
6	0.00	0.00	0.08	0.00	0.42	0.00	0.50	0.00	0.00	0.00
7	0.00	0.00	0.17	0.50	0.00	0.00	0.00	0.25	0.08	0.00
8	0.00	0.00	0.17	0.08	0.08	0.00	0.00	0.00	0.58	0.08
9	0.00	0.08	0.00	0.17	0.17	0.00	0.08	0.00	0.25	0.25

Figure 3. HOG: After Blur

digit	0	1	2	3	4	5	6	7	8	9
0	0.25	0.00	0.08	0.00	0.00	0.00	0.67	0.00	0.00	0.00
1	0.00	0.50	0.00	0.17	0.08	0.00	0.00	0.25	0.00	0.00
2	0.00	0.00	0.67	0.17	0.00	0.00	0.08	0.00	0.08	0.00
3	0.00	0.00	0.00	0.58	0.08	0.00	0.25	0.00	0.08	0.00
4	0.00	0.00	0.00	0.25	0.75	0.00	0.00	0.00	0.00	0.00
5	0.00	0.00	0.00	0.00	0.00	0.42	0.42	0.00	0.17	0.00
6	0.00	0.00	0.00	0.00	0.50	0.00	0.42	0.00	0.08	0.00
7	0.00	0.00	0.25	0.42	0.08	0.00	0.00	0.25	0.00	0.00
8	0.00	0.00	0.17	0.08	0.08	0.00	0.00	0.00	0.67	0.00
9	0.00	0.08	0.00	0.17	0.17	0.08	0.08	0.00	0.17	0.25

Figure 4. HOG: After Gamma Correction

digit	0	1	2	3	4	5	6	7	8	9
0	0.25	0.00	0.00	0.00	0.00	0.00	0.67	0.00	0.00	0.08
1	0.33	0.25	0.00	0.00	0.00	0.00	0.00	0.00	0.33	0.08
2	0.00	0.08	0.42	0.17	0.00	0.00	0.00	0.00	0.33	0.00
3	0.08	0.00	0.00	0.33	0.00	0.00	0.00	0.00	0.33	0.25
4	0.08	0.00	0.00	0.17	0.42	0.00	0.08	0.00	0.17	0.08
5	0.00	0.00	0.00	0.17	0.08	0.17	0.33	0.00	0.17	0.08
6	0.00	0.00	0.08	0.00	0.08	0.00	0.33	0.00	0.50	0.00
7	0.08	0.00	0.08	0.25	0.00	0.00	0.00	0.08	0.50	0.00
8	0.17	0.00	0.08	0.08	0.00	0.00	0.08	0.00	0.50	0.08
9	0.08	0.00	0.00	0.33	0.08	0.08	0.08	0.00	0.17	0.17

Figure 5. HOG: After Sharpening

digit	0	1	2	3	4	5	6	7	8	9
0	0.00	0.25	0.08	0.17	0.00	0.00	0.42	0.00	0.08	0.00
1	0.00	0.50	0.00	0.50	0.00	0.00	0.00	0.00	0.00	0.00
2	0.00	0.08	0.42	0.25	0.00	0.00	0.17	0.00	0.08	0.00
3	0.00	0.00	0.00	0.42	0.00	0.08	0.50	0.00	0.00	0.00
4	0.00	0.00	0.08	0.33	0.42	0.00	0.08	0.00	0.08	0.00
5	0.00	0.00	0.00	0.08	0.08	0.25	0.42	0.00	0.08	0.08
6	0.00	0.00	0.00	0.17	0.00	0.00	0.50	0.00	0.33	0.00
7	0.00	0.17	0.08	0.25	0.08	0.00	0.08	0.00	0.33	0.00
8	0.00	0.08	0.17	0.08	0.08	0.00	0.25	0.00	0.25	0.08
9	0.00	0.08	0.08	0.25	0.17	0.00	0.33	0.00	0.08	0.00

Figure 6. HOG: After Rotation

KNOWN	0	1	2	3	4	5	6	7	8	9
0	0.17	0.00	0.00	0.00	0.50	0.00	0.33	0.00	0.00	0.00
1	0.00	0.58	0.00	0.00	0.42	0.00	0.00	0.00	0.00	0.00
2	0.00	0.00	0.25	0.00	0.08	0.25	0.25	0.17	0.00	0.00
3	0.00	0.08	0.25	0.08	0.17	0.17	0.17	0.08	0.00	0.00
4	0.00	0.00	0.00	0.00	0.67	0.00	0.25	0.08	0.00	0.00
5	0.00	0.00	0.25	0.00	0.25	0.00	0.33	0.17	0.00	0.00
6	0.00	0.00	0.00	0.00	0.58	0.08	0.08	0.25	0.00	0.00
7	0.00	0.00	0.00	0.00	0.25	0.17	0.08	0.50	0.00	0.00
8	0.08	0.00	0.08	0.08	0.17	0.17	0.08	0.33	0.00	0.00
9	0.17	0.00	0.00	0.00	0.17	0.00	0.42	0.25	0.00	0.00

Figure 7. SURF: Before Transformation

KNOWN	0	1	2	3	4	5	6	7	8	9
0	0.08	0.00	0.17	0.08	0.25	0.17	0.17	0.08	0.00	0.00
1	0.08	0.25	0.00	0.00	0.67	0.00	0.00	0.00	0.00	0.00
2	0.17	0.00	0.08	0.17	0.00	0.08	0.25	0.25	0.00	0.00
3	0.00	0.17	0.58	0.00	0.00	0.08	0.08	0.00	0.08	0.00
4	0.00	0.00	0.00	0.08	0.50	0.17	0.25	0.00	0.00	0.00
5	0.08	0.00	0.42	0.00	0.17	0.08	0.08	0.08	0.08	0.00
6	0.00	0.08	0.00	0.00	0.67	0.17	0.08	0.00	0.00	0.00
7	0.08	0.00	0.17	0.08	0.33	0.08	0.00	0.25	0.00	0.00
8	0.00	0.00	0.08	0.08	0.33	0.17	0.08	0.17	0.00	0.08
9	0.17	0.00	0.25	0.08	0.17	0.00	0.17	0.08	0.00	0.08

Figure 8. SURF: After Blur

KNOWN	0	1	2	3	4	5	6	7	8	9
0	0.25	0.00	0.00	0.00	0.17	0.08	0.33	0.17	0.00	0.00
1	0.00	0.33	0.00	0.00	0.08	0.00	0.00	0.58	0.00	0.00
2	0.00	0.08	0.08	0.08	0.00	0.17	0.42	0.17	0.00	0.00
3	0.08	0.08	0.00	0.08	0.25	0.17	0.08	0.17	0.08	0.00
4	0.00	0.08	0.00	0.00	0.33	0.00	0.50	0.08	0.00	0.00
5	0.00	0.00	0.08	0.08	0.08	0.00	0.33	0.42	0.00	0.00
6	0.00	0.08	0.00	0.00	0.50	0.00	0.25	0.17	0.00	0.00
7	0.00	0.00	0.00	0.00	0.17	0.00	0.17	0.67	0.00	0.00
8	0.08	0.08	0.00	0.00	0.33	0.25	0.08	0.17	0.00	0.00
9	0.25	0.00	0.00	0.00	0.17	0.25	0.08	0.25	0.00	0.00

Figure 9. SURF: After Gamma Correction

KNOWN	0	1	2	3	4	5	6	7	8	9
0	0.17	0.00	0.00	0.08	0.33	0.08	0.33	0.00	0.00	0.00
1	0.50	0.00	0.00	0.00	0.50	0.00	0.00	0.00	0.00	0.00
2	0.17	0.08	0.00	0.25	0.00	0.17	0.25	0.08	0.00	0.00
3	0.00	0.00	0.25	0.17	0.17	0.33	0.00	0.08	0.00	0.00
4	0.08	0.00	0.00	0.00	0.58	0.00	0.33	0.00	0.00	0.00
5	0.00	0.00	0.08	0.25	0.17	0.25	0.17	0.08	0.00	0.00
6	0.00	0.08	0.00	0.00	0.58	0.00	0.33	0.00	0.00	0.00
7	0.00	0.08	0.00	0.08	0.25	0.00	0.08	0.50	0.00	0.00
8	0.25	0.00	0.08	0.00	0.25	0.17	0.17	0.08	0.00	0.00
9	0.17	0.08	0.00	0.08	0.25	0.08	0.25	0.08	0.00	0.00

Figure 10. SURF: After Sharpening

KNOWN	0	1	2	3	4	5	6	7	8	9
0	0.00	0.50	0.00	0.00	0.00	0.00	0.50	0.00	0.00	0.00
1	0.00	1.00	0.00	0.00	0.00	0.00	0.00	0.00	0.00	0.00
2	0.00	0.25	0.00	0.00	0.00	0.00	0.75	0.00	0.00	0.00
3	0.00	0.83	0.00	0.00	0.00	0.00	0.17	0.00	0.00	0.00
4	0.00	0.92	0.00	0.00	0.00	0.00	0.08	0.00	0.00	0.00
5	0.00	0.75	0.00	0.00	0.00	0.00	0.08	0.08	0.00	0.08
6	0.00	0.75	0.00	0.00	0.00	0.00	0.25	0.00	0.00	0.00
7	0.00	0.92	0.00	0.00	0.00	0.00	0.08	0.00	0.00	0.00
8	0.00	0.75	0.00	0.00	0.00	0.00	0.25	0.00	0.00	0.00
9	0.00	0.92	0.00	0.00	0.00	0.00	0.08	0.00	0.00	0.00

Figure 11. SURF: After Rotation

IV. Results And Discussions

A. USING HOG FEATURES

a) Before Transformations : Figure 2. Shows the confusion matrix obtained on the classifier before applying Transformation. Relatively less error rates are obtained. Misclassification can be seen in 0 where 0 has been mostly classified as 6.Similar errors are seen in 6 and 5.The above confusion matrix has an average accuracy of 0.49.

b) After Transformations :

- Results for blur: The columns of the confusion matrix in Figure 3 represent predicted labels and the rows of represent known labels. From the confusion matrix it i s evident that 0 has often been misclassified as 6, since blurring the images of 6 seems similar to 0. Simi larly ,6 and 7 are also misclassified as 8. The average accuracy is 0.29.
- Results for gamma: Figure. 4. illustrates the confusion matrix for gamma transformation. It is evident that 7 have been misclassified often as 3. Similarly, there are errors in 0. The average accuracy is 0.48.
- Results for sharpen: Figure 5. shows the confusion matrix obtained after the sharpen transformation has been applied. The average accuracy is 0.48. It shows relatively lesser misclassification compared to other transformations. But here there is also a misclassification of 0 as 6.
- Results for rotation: The representation of the confusion matrix in Figure.6 shows that 1 has been often misclassified as 3, whereas 3 has been misclassified as 6. Also there has been misclassification of 7 as 8 after rotation and 5 as 6 after rotation. The average accuracy is only 0.28.

B. USING SURF FEATURES

a) Before Transformations : It shows that misclassification rates are comparatively less compared to those extracted using HOG features. But still there is some misclassification in 9, 6 and 5.Confusion Matrix shown in Figure 7 depicts that

b) After transformations

- Results for blur: Figure 8 shows Confusion matrix ob tained after applying blur transformation is shown in fig. 8. 1 and 6 is misclassified as 4. It is due to the distortion in image due to blurring; the classifier is unable to detect the right images.
- Results for gamma: Figure 9 shows the confusion matrix after applying gamma correction on the images. The accuracy obtained is 0.20 which is approximately equal to the confusion matrix obtained before applying transformations. Here, errors in misclassification is less.1 is often misclassified as 7 and similarly for 4 which is misclassified as 6.
- Results for sharpen: Figure 10 shows confusion matrix for sharpen transformation. Misclassification is seen in 6 where 6 has been misclassified as 4. Also 1 has been classified as 6 mostly
- Results for rotation: Figure 11 is the confusion matrix for rotation transformation. It shows a major misclassification for 1 where 4, 7 and 9 have been misclassified as 1. Similar errors can be seen in 6 and 8. There is a perfect classification for 1

CONCLUSION

From the experiments it can be concluded that SVM is highly vulnerable to evasion attacks. From the HOG feature extraction and SURF feature extraction it is found that digit images extracted using HOG features are more vulnerable to image transformations like blurring, sharpening and rotation. SURF is proved to be invariant to transformations like rotation, blur, sharpening while HOG is not invariant. HOG has an average accuracy of 0.49 before applying transformations. It was found that after applying transformations, the average accuracy got reduced. But, it can be concluded that, sharpen and gamma transformations show very less deviation (0.48) from the trained average accuracy of HOG. Similarly, in SURF ,the average accuracy obtained before applying transformations is 0.23.The accuracies obtained after applying transformations reduced. An overall analysis shows that blur and rotation transformations are stronger in making the SVM vulnerable. In adversarial settings, smart and adaptive adversaries can deliberately manipulate data (violating stationarity) to exploit existing learning algorithm vulnerabilities and impair the entire system. This raises several open questions concerning whether machine-learning techniques can be used safely in security-sensitive tasks.

REFERENCES

[1] N. Dalal and B. Triggs(2005), Histograms of Oriented Gradients for Human Detection, Proc. IEEE Conf. Computer Vision and Pattern Recognition, Vol. 1, 886-893.

[2] Bristow, Hilton, and Simon Lucey. "Why do linear SVMs trained on HOG features perform so well?." arXiv preprint arXiv:1406.2419 (2014).

[3] S. Tong and D. Koller (2000) Support vector machine active learning with applications to text classification, ICML

[4] D. G. Lowe (1999) Object Recognition from local scale invariant features, ICCV (International Conference on Computer Vision).

[5] Bay, Herbert, Tinne Tuytelaars, and Luc Van Gool. "Surf: Speeded up robust features." In European conference on computer vision, pp. 404-417. Springer, Berlin, Heidelberg, 2006.

[6] Kurakin, Alexey, Ian Goodfellow, and Samy Bengio. "Adversarial machine learning at scale." arXiv preprint arXiv:1611.01236 (2016)

[7] Huang, Ling, Anthony D. Joseph, Blaine Nelson, Benjamin IP Rubinstein, and J. D. Tygar. "Adversarial machine learning." In Proceedings of the 4th ACM workshop on Security and artificial intelligence, pp. 43-58. ACM, 2011.

[8] Guo, C., Rana, M., Cisse, M. and Van Der Maaten, L., 2017. Countering adversarial images using input transformations. arXiv preprint arXiv:1711.00117.

Second International Conference on Smart Systems and Inventive Technology (ICSSIT 2019)
IEEE Xplore Part Number: CFP19P17-ART; ISBN:978-1-7281-2119-2

POS Tagger for Malayalam using Hidden Markov Model

Sindhya K Nambiar
Asst. Professor, Computer Science and Engineering,
SCMS School of Engineering and Technology,
Karukutty, Ernakulam, India
sindhyak@yahoo.com

Antony Leons
SCMS School of Engineering and Technology,
Karukutty, Ernakulam, India

Soniya Jose
Asst. Professor, Computer Science and Engineering,
SCMS School of Engineering and Technology,
Karukutty, Ernakulam, India

Arunsree
SCMS School of Engineering and Technology,
Karukutty, Ernakulam, India

***Abstract*—The NLP applications uses the parts of speech tagging as the preprocessing step. For making POS tagging accurate, various techniques have been explored. But in Indian languages, not much work has been done. This paper describes Part of Speech Tagger by incorporating Hidden Markov Model is built. Supervised learning approach is implemented in which, already tagged sentences in Malayalam is used to build Hidden Markov Model.**

Keywords—Hidden Markov-model; POS tagging; Supervised learning; Malayalam language; rule based taggers; stochastic taggers.

I. INTRODUCTION

Linguistic processing uses Part of Speech (POS) as a feature to translate the sentences. A POS Tagger is a translator that takes the sentences and outputs the word sequences with its part of speech tags. Tagger examines each word with its context in the sentence during the analysis process.

Part of Speech Tagging, which is a grammatical tagging tagged the words in a text based on its context and definition. The POS tagging is useful in many research areas includes Speech Recognition, Information Retrieval, Speech Synthesis etc. In English, lots of works has been done in part of speech tagging. But unfortunately, in regional languages not much has been done especially in Malayalam. As the structure of Indian languages differs from the Western languages, the existing taggers cannot be used for Indian languages. Hence the rule-based taggers would not work well in this scenario whereas the stochastic taggers can be used in a very crude form. With some knowledge on the structure of the language these taggers give better results.

A Hidden Markov Model (HMM), which is a statistical model is the system modeled as a Markov process with the unknown parameters[2]. The probability of the word in a sequence might depend on the word preceding it immediately, with the hidden and the observed words coming successively in a sentence. Based on the above assumption, the model is prepared by observing various scenarios. In POS tagging, the tags cannot be seen but the words are visible. This favors the use of HMM to model the system, as it allows observed words in input sentence and hidden tags to be built into it with each of the hidden tag state produces a word in a sentence.

Viterbi algorithm, a popular search algorithm is used for lexical calculations in HMM. This is a dynamic programming algorithm which results in a sequence of the observed words. This algorithm implements the n-grams approach, and it works based on the number of assumptions it makes. The algorithm is based on the assumption that at a given instant of time, both the hidden and the observed word must form a sequence. Moreover, It expects that the tag sequence to be aligned. This algorithm calculates the most likely tag sequence that can occur which is unambiguous and unique, until the correct tag is obtained. At each level most appropriate sequence and the probability including these are computed.

Since Malayalam is a morphological rich language, each word may come up with different tags for different sentences. And also POS tagging is very useful to pre-process the documents for similarity checking , summary generation etc.

II. RELATED WORKS

Tagger with the highest possible accuracy is required for language processing. In usual cases accuracy of Statistical approach is better compared to Rule based Approach. Parts-of-speech tagging has good practical application, with uses in many areas, including machine translation, parsing, information retrieval and lexicography. Initially with the aid of a corpus people engineered rule for tagging. Later, with the support of large corpus, Markov-model based stochastic taggers which were trained automatically gives highly accurate tagging result [1].

Two approaches are there in POS tagging: rule-based approach and stochastic approach. Rule based taggers [2] make use of considerably large database of words which have predefined disambiguation rule. Consider the example, that an ambivalent word is a verb or a noun. Stochastic taggers use statistical algorithm along with training corpus to check for the ambivalence. One of the oldest approach in tagging is Rule based approach, which use predefined rules. The prior algorithms for assigning parts-of-speech automatically can be traced back to a two-stage architecture. The Initial stage uses a dictionary to label word. The second stage make use of large lists of already defined disambiguation rules to labeling word precisely. They take less storage and use simple rules. Rule based taggers make use of morphological statistics along with predefined rule to designate tags to unknown or ambivalent words. Stochastic approach makes use of statistical information and probability for assigning tag to words. This approach uses statistical algorithms as alternative to grammar rule. They are predominantly more precise when compared to rule based taggers. Stochastic taggers are commonly used because of their higher degree of precision when compared to the rule based taggers.

In other words, high accuracy is acquired using some complex procedures and data structures. HMMs Stochastic grammars and HMMS are generic models, allocating a joint probability to the label sequences and paired observation; the specifications are normally trained to magnify the joint probability of training examples [4]. An usual model list all attainable observation sequences requiring a depiction to define a joint likelihood over label sequences and observation. In particular, it is not realistic to entitle long range dependencies. This difficulty is one of the main motivating forces for looking at conditional models as a substitute.

Considerable progress has been made in the estimation of models with latent variables in recent years. Even with NP-hardness in general cases [7]. Various approaches to solve one of the classical problems of unsupervised learning involving the Unsupervised POS tagging has been addressed in [4].

III PROPOSED METHODOLOGY

The fig .1 provides the proposed architecture, it performs the following functions: It takes an input sentence in Malayalam Language; it processes the input text and computes the transition and emission probabilities. The probabilities computed are then stored in a 2-D matrix in the form of an intermediate file, which is then given to Viterbi Algorithm to find the best POS sequence for the input.

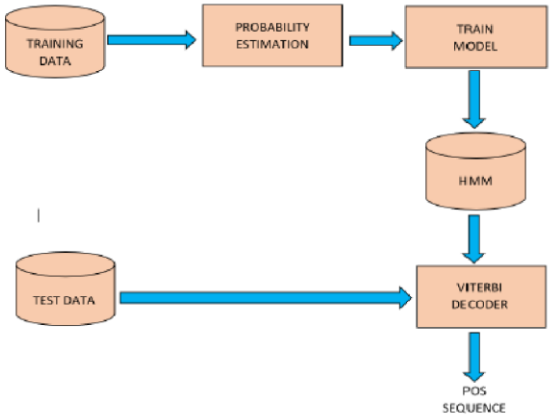

Fig. 1. Block diagram of proposed system

Hidden Markov Model is used to find the optimal probable tag sequence.

A. Hidden Markov Model for POS tagging

The Hidden Markov Model makes use of two different kinds of probabilities[4]. They are: POS transition probabilities and Word emission probabilities. The transition probability is the occurrence of a new tag from the current tag in the input. Learning Markov models (with tags) is started by counting the number of occurrences in the corpus and then followed by determining the probability be dividing with context. The instinct behind HMM and the stochastic taggers is the "pick the most likely tag for this word" approach. HMM taggers use the tag sequence that maximizes the formula (1) for a word sequence or given sentence.

"P (word | tag) * P (tag | previous n tags)". (1)

For identifying the maximum probability in the HMM it uses the Viterbi Algorithm

3.1.1. Viterbi for POS tagging
Input: sentence
Initialize a map for the transition, possible_tags, emission, in the model file.
Split the line based on the type,word, context an prob

FORWARD STEP: The lines are split into the words.
And the scores are reviewed
BACKWARD STEP:
Adds the substrings and combines the tags into a string and print

Enumerate the sentence transition initially followed by the score enumeration of the existing and the forth coming sentence and ends the sentence with the final symbol.

A. POS tag set

.The tag set developed for the work is given in Table1.

SL.NO.	TAGS	DESCRIPTION
1	<NN>	NOUN
2	<NNC>	COMPOUND NOUN
3	<NNP>	PROPER NOUN
4	<PRP>	PRONOUN
5	<ADJ>	ADJECTIVE
6	<ADV>	ADVERB
7	<CNJ>	CONJUNCTION
8	<VN>	VERBAL NOUN
9	<Q>	QUANTIFIER
10	<DET>	DETERMINERS
11	<PSP>	POST POSITIONS
12	<RP>	PARTICLES
13	<RD_PUNC>	PUNCTUATIONS

Table 1. POS Tag set

III. EXPERIMENTAL RESULTS

In the experimental phase of the system development, around two hundred sentences are used to train the model. The system was trained using the corpus which is already tagged.. the test data set are utilized in testing the system and the lexical generation probability and the emission probability were used to tag the data set used for testing. The results shown below were obtained while testing the test data. By increasing the number of sentences in training set, tagging system accuracy is improved upto 85%. Only 13 tag sequences are used for performance, and the result obtained from was very satisfactory.

Some of the outputs are shown below

Input sentence1:

□□□.

Tagged sentence:

□□□□□□□□\PR_PRP □□□□□□□□□□□\N_NN
□□□□□□□□□□□□□□□□□□□□□□□□□\N_NN
□□□□□□□□□□□□□□□□□□\N_NN □□□□□□□□□\N_NN
□□□□□□□□□□□□□□□□□□\N_NN
□□□□□□□□□□□□□□□□□□□□\N_NN
□□□□□□□□\V_VN□□□□□□□□□□□□□□□□□□□□ \
V_VN .\RD_PUNC

Input sentence2:

□□

Tagged sentence:

□□□□□□□□□□□□□□□□□\N_NN
□□□□□□□□□□□□□\N_NN
□□□□□□□□□□□□□□□□□□□□□□□□\N_NN □\DM_DMD
□□□□□□□□□□□□□□□\N_NN
□□□□□□□□□□□□□□□□□□□□□□□□□□\V_VN

Input sentence3:

□□□□□□□□□□□□□□□□□ □□□ □□□□□□□□□□□□□□□□□□□□□□□□□ □□□□□□□□□□□□

Tagged sentence:

□□□□□□□□□□□□□□□□□□□\N_NN
□□□□□□□□□□□□□□□□□□□□□□\V_VN
□□□□□□□□□□□□□□□□□□□□□□□□□□\N_NN
□□□□□□□□□□□□□□□□□□□□□□□□\N_NN □\DM_DMD
□□□□□□□□□□□□\N_NN □□□□□□□□□□□□□□\N_NNP
□□□□□□□□□□□\V_VN

IV. CONCLUSION

Hidden markov model is a good way of doing POS tagging for Malayalam sentences. The system successfully trained and tested a POS tagger on a considerable sized dataset and demonstrated its abilities to discern context as well as classify POS accurately.

V. REFERENCES

[1] Jayan, Jisha P., and R. R. Rajeev. "Parts Of Speech Tagger and Chunker for Malayalam–Statistical Approach." *Computer Engineering and Intelligent Systems* 2.2 (2011): 68-78.

[2] Antony, P. J., and K. P. Soman. "Parts of speech tagging for Indian languages: a literature survey." International Journal of Computer Applications 34.8 (2011): 0975-8887.

[3] Bellegarda, Jerome R. "Part-of-speech tagging by latent analogy." IEEE Journal of Selected Topics in Signal Processing 4.6 (2010): 985-993.

[4] Stratos, Karl, Michael Collins, and Daniel Hsu. "Unsupervised part-of-speech tagging with anchor hidden markov models." Transactions of the Association for Computational Linguistics 4 (2016): 245-257.

[5] Anandkumar, Animashree, Daniel Hsu, and Sham M. Kakade. "A method of moments for mixture models and hidden Markov models." Conference on Learning Theory. 2012.

[6] Merialdo, Bernard. "Tagging English text with a probabilistic model." Computational linguistics 20.2 (1994): 155-171.

[7] Terwijn, Sebastiaan A. "On the learnability of hidden Markov models." International Colloquium on Grammatical Inference. Springer, Berlin, Heidelberg, 2002.

[8] Hsu, Daniel, Sham M. Kakade, and Tong Zhang. "A spectral algorithm for learning hidden Markov models." Journal of Computer and System Sciences 78.5 (2012): 1460-1480.

[9] Haghighi, Aria, and Dan Klein. "Prototype-driven learning for sequence models." Proceedings of the main conference on Human Language Technology Conference of the North American Chapter of the Association of Computational Linguistics. Association for Computational Linguistics, 2006.

[10] Berg-Kirkpatrick, Taylor, et al. "Painless unsupervised learning with features." Human Language Technologies: The 2010 Annual Conference of the North American Chapter of the Association for Computational Linguistics. Association for Computational Linguistics, 2010.

[11] Johnson, Mark. "Why doesn't EM find good HMM POS-taggers?." Proceedings of the 2007 Joint Conference on Empirical Methods in Natural Language Processing and Computational Natural Language Learning (EMNLP-CoNLL). 2007.

[12] Ekbal, Asif, S. Mondal, and Sivaji Bandyopadhyay. "POS Tagging using HMM and Rule-based Chunking." The Proceedings of SPSAL 8.1 (2007): 25-28.

[13] Sunitha, C. "A hybrid Parts Of Speech tagger for Malayalam language." 2015 International Conference on Advances in Computing, Communications and Informatics (ICACCI). IEEE, 2015.

Controllability studies on fish-shaped unmanned under water vehicle undergoing manoeuvring motions

Conference Paper · September 2019

DOI: 10.1201/9780367810085-

6 authors, including:

Ak Ranjith
SCMS Group of Educational Institutions
6 PUBLICATIONS **9** CITATIONS
SEE PROFILE

Sheeja Janardhanan
Indian Maritime University
66 PUBLICATIONS **77** CITATIONS
SEE PROFILE

Vidya Chandran
SCMS School of Engineering and Technology, Karukutty
24 PUBLICATIONS **31** CITATIONS
SEE PROFILE

Noel Gomez
SCMS Group of Educational Institutions
4 PUBLICATIONS **2** CITATIONS
SEE PROFILE

Controllability studies on fish-shaped unmanned under water vehicle undergoing manoeuvring motions

A. K. Ranjith, S. Janardhanan, V. Chandran & N. J. Gomez
Department of Mechanical Engineering, SCMS School of Engineering and Technology, Ernakulam, India

G. Ilieva
Department of Ship Building, Technical University of Varna, Bulgaria

J. Sygal
Department of Ocean Engineering, Indian Institute of Technology Madras, India

ABSTRACT: Bio-inspired propulsion systems have many advantages over the conventional ones. They are found to be noiseless and eco-friendly. Most of the aquatic locomotion makes use of oscillations, paddling and water-jet for producing net thrust on the body. In this paper a box-fish shaped unmanned underwater vehicle (UUV) has been considered for studying its controllability. A RANS based CFD method has been implemented for simulating manoeuvring motions in heave and pitch to obtain the forces and moments during such motions.

1 INTRODUCTION

Bio-inspired propulsion is a much researched field these days. The fact that, the noise and vibrations produced during the operation of conventional propellers have adversely affected the bio-diversity of oceans, has made bio-inspired propulsion more enticing to mankind. Getting rid of the conventional rotary components of a propulsion system completely is also not practical. Ocean transport do contribute to a mammoth scale of world's economy. Hence there should be a balance between bio-inspired flapping foil as well as the conventional propulsion systems so that we do not tamper much with the ecological systems and at the same time do contribute to the economy.

Nature is known as the master engineer. The efficiency of propulsion of some aquatic animals have struck us in awe and the values of their efficiency have far outperformed those of man-made vehicles. Now it is time to have a few such vehicles operating in the oceans. There have been many studies in the past decades concentrating on the flapping foil mechanisms on ocean vehicles: both surface and sub-sea. Most of them focused on the determination of propulsive efficiency while others on the controllability.

1.1 *Understanding the locomotion of fish*

The locomotion of the fish is indeed complex yet efficient. Various fins involved in the locomotion or swimming are shown in Figure 1.

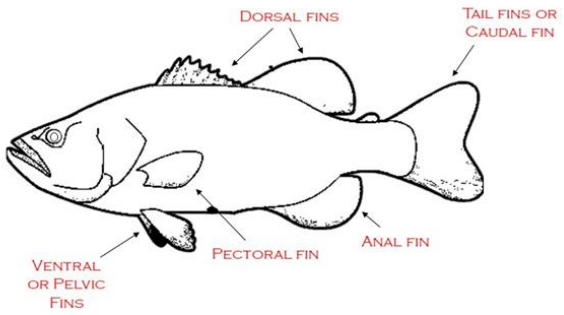

Figure 1: Various fins on the body of a fish

Fishes swim using all the fins. The locomotion a fish swimming with tail fin or the caudal fin and the trunk is broadly classified into angulliform, subcarangiform, carangiform, thunniform and ostraciiform (Figure 2). From angulliform to ostraciiform the locomotion gets simplified with the deteriorating involvement of the trunk as the undulations of the entire trunk reduces to mere oscillations of the tail during swimming. Locomotion of the fish with varying involvement of the trunk and tail is shown in Figure 3.

In ostraciiform models, the undulation is confined mostly to the caudal fin without moving the body. The thrust for this model is generated with a lift-based method, allowing cruising speeds to be maintained for long periods. This form is considered to be the sim-

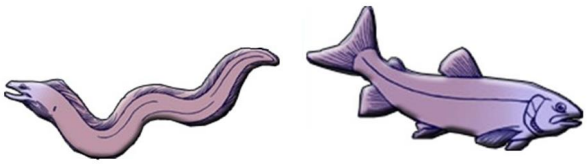

(a) Angulliform (eel)

(b) Carangiform (salmon)

(c) Thunniform (tuna)

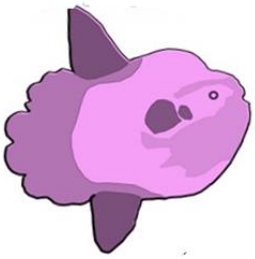

(d) Ostraciiform (sunfish)

Figure 2: Fish with different types of tail locomotion

plest of all for carrying out mathematical studies. A UUV with hull form geometrically similar to that of a box-fish, a typical ostraciiform model undergoing manoeuvring motions in heave and pitch, has been analysed for controllability in the present study. UUVs also known as underwater drones are vehicles with no humans onboard during the course of their mission. There are basically two types of UUVs- autonomous underwater vehicle (AUV) and remotely operated vehicle (ROV). AUVs are more or less like robots not entailing human intervention throughout their mission while ROVs are remotely operated from a ground station.

In the case of present work, the vehicle's hull form is more important than its mode of operation. Guidance and control are very important aspects in the design of marine vehicles no matter whether they are surface or underwater vehicles. A motion planning and control system was developed for autonomous surface vehicles by Hinostroza, Guedes Soares, & Xu 2018. This work aims at achieving the first step in controllability predictions-determination of forces and moments during manoeuvring motions. A linear mathematical model combined with a RANS based CFD method has been used for obtaining the thrust generated during the oscillatory motions of the tail with ANSYS FLUENT as the solver. The forces and moments acting on the hull form in both static and dynamic manoeuvres have been estimated. This paper is an initial step towards the controllability and stability prediction of fish-shaped UUVs which could be used in search and rescue as well as surveillance missions. Hence it is imperative to predict the trajectory of such vessels well in advance through controllability studies of its hull form.

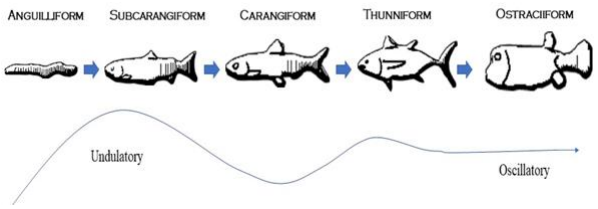

Figure 3: Undulatory motion of the entire trunk to oscillatory motion of the tail

It is quite evident that the ostraciiform type of locomotion is the simplest mode of locomotion. A design based on this type of locomotion will be obviously the most feasible for a UUV. The studies on ostraciiform type of locomotion was reported by Blake 1977. The study made some interesting observations. For slow progression, the caudal fin inclination with the longitudinal axis of the body is about 3 to 6 deg while for fast progression, the angle is 35 deg. 3-D manoeuvring studies were carried out on a fish-like robot by Wu, Yu, Su, & Tan 2014. The robotic fish here was fabricated using multi-link joints to obtain the agility during swimming and hence better manoeuvrability. The present study considers the controllability aspects of a box-fish by numerically simulating the manoeuvring motions.

Not much work has been reported on the determination of hydrodynamic derivatives of the body form for assessing the vesselś controllability. This paper presents a method for numerically evaluating the hydrodynamic forces and moments-an initial step towards the estimation of hydrodynamic derivatives and thereby the controllability of a box-fish shaped underwater vehicle.

2 UUV GEOMETRY

A box fish in its three dimensional configuration is shown in Figure 4. The principal particulars of the fish are given in Table 1.

Table 1: Principal particulars of the UUV

Dimension	Size (metres)
Length (L)	1.3
Breadth (B)	0.5
Depth (D)	0.5

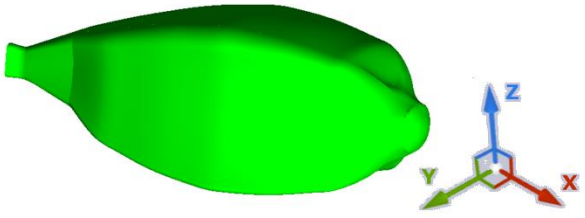

Figure 4: Three dimensional representation of the box-fish shaped UUV

3 MATHEMATICAL MODEL

The Cartesian co-ordinate system of the UUV is shown in Figure 5. The conventional North-East-Down (NED) system is followed here.

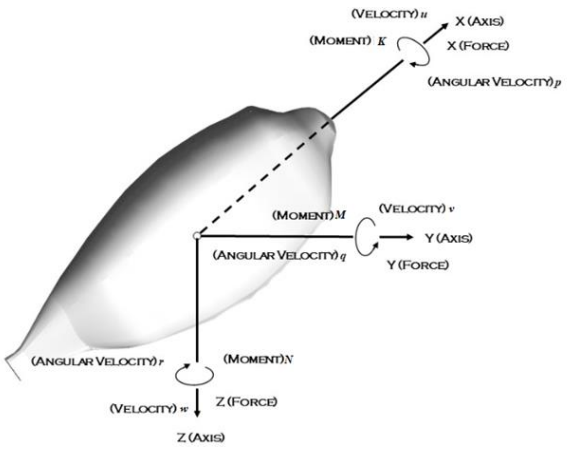

Figure 5: Co-ordinate system used in the study

A linear mathematical model describing the manoeuvring motions of the UUV is represented by Equations (1) through (6)

$$X = X_{\dot{u}}\dot{u} + X_{u|u|}u^2 + X_w w + X_q q + X_\delta \delta + X_T \quad (1)$$

$$Y = Y_{\dot{v}}\dot{v} + Y_v v + Y_p p + Y_r r + Y_\delta \delta \quad (2)$$

$$Z = Z_{\dot{w}}\dot{w} + Z_w w + Z_u u + Z_q q + Z_\delta \delta \quad (3)$$

$$K = K_{\dot{p}}\dot{p} + K_p p + K_v v + K_r r + K_\delta \delta \quad (4)$$

$$M = M_{\dot{q}}\dot{q} + M_q q + M_w w + M_u u + M_\delta \delta \quad (5)$$

$$N = N_{\dot{r}}\dot{r} + N_r r + N_v v + N_p p + N_\delta \delta \quad (6)$$

where subscript T represents thrust and δ, the rudder angle.

4 NUMERICAL EVALUATION OF CONTROLLABILITY IN VERTICAL PLANE

4.1 *Numerical Modelling and Meshing*

For studying the hydrodynamic forces and moments on the UUV during manoeuvring motion there are two basic methods, viz. numerical and experimental. While experimental methods involve prohibitively expensive and rare facilities, numerical methods offer the ease of bringing tedious tasks to desks. However numerical methods have not yet become self sufficient to completely replace experiments. They definitely offer promising inputs to the conceptual design. In this paper an attempt has been made to simulate

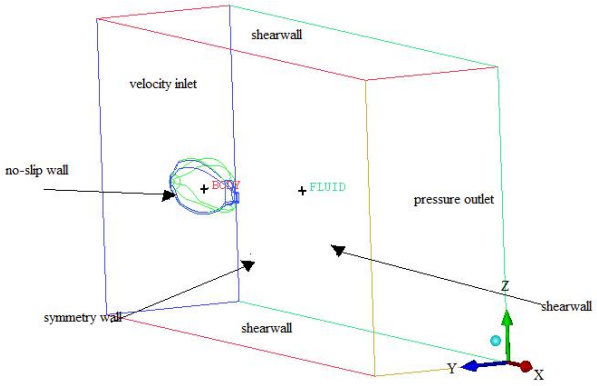

Figure 6: Computational domain with its boundaries

the manoeuvring motions in the vertical plane of the UUV's motions.

Geometric modelling and meshing has been carried out using the commercial package ANSYS ICEM CFD. Figure 6 shows the computational domain. Its extends are $2.0L \leq x \leq 5.0L$, $2.0L \leq y \leq 2.0L$ and $0 \leq z \leq 2.0L$.

An unstructured meshing strategy is employed here. The minimum cell size has been calculated following the method described by Chandran, Janardhanan, Menon, et al. 2018.

Boundary layer thickness and the near wall element size have been calculated from boundary layer theory. The thickness of laminar sub-layer is obtained from Equation (7) (Schlichting & Gersten 2016).

$$\delta' = \frac{11.6v}{V^*} \quad (7)$$

where V^* is the frictional velocity given by Equation (8)

$$V^* = \sqrt{\frac{\tau_0}{\rho}} \quad (8)$$

and τ_0 , the wall shear stress, is obtained as in Equation (9).

$$\tau_0 = \frac{0.664}{\sqrt{Re_L}} \cdot \frac{\rho V^2}{2} \quad (9)$$

where, V is the flow velocity and Re_L the length based Reynolds number.

The mesh generated in the computational domain in shown in Figure 7(a). The magnified view around the fish body is shown in figure 7(b).

A velocity corresponding to $Re = 0.5 \times 10^6$ is imposed on the velocity inlet. The outlet is considered to be a pressure outlet. Half-fish model is used with the plane holding mid x-y plane as a symmetry wall. Non-slip boundary condition is assigned to the UUV body and slip walls to the far-field.

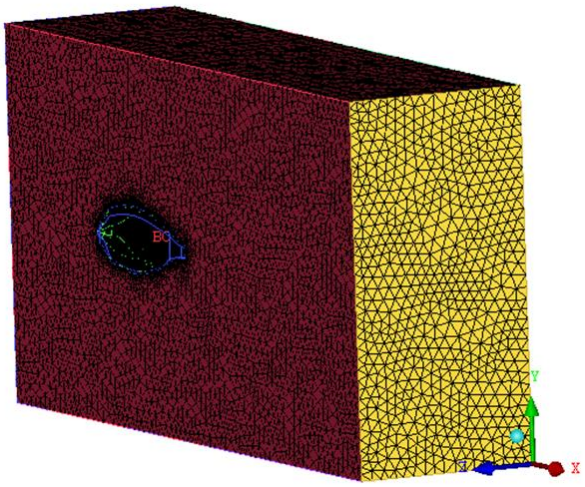

(a) Mesh in the domain

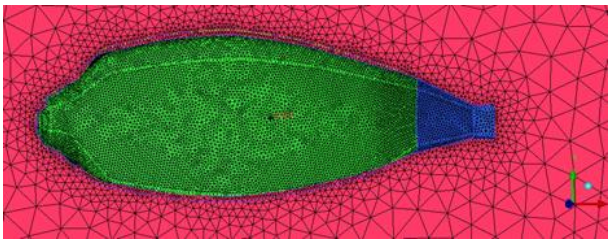

(b) Magnified view around the UUV body

Figure 7: Unstructured mesh for computation

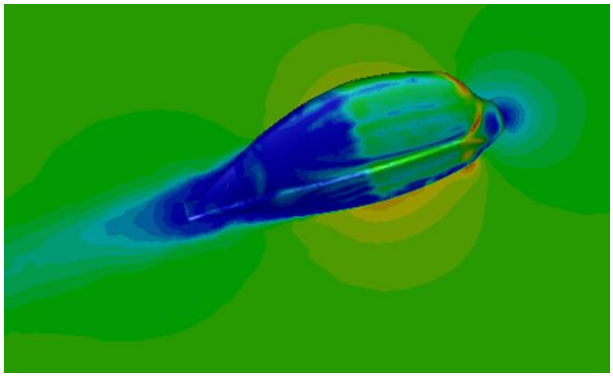

Figure 8: Dynamic pressure contours on the half-UUV

4.2 *Steady-state predictions*

Steady simulations are carried out with $k-\omega$ SST two equation model. PISO scheme is used for pressure velocity coupling. The convergence criteria is set to 10^{-7}. The simulations have been carried out using ANSYS FLUENT version 18.1. Dynamic pressure contours on the half-fish model is shown in Figure 8.

4.3 *Static manoeuvre simulations*

As the 3D simulations were time consuming, for faster predictions, a cut section of the UUV in the 2D plane is used for further analysis. The coefficients of drag (C_D) and lift (C_L) obtained from 3D simulations discussed in the previous section have been used as the reference. The challenge in 2D CFD simulations to yield results close to 3D simulations lies in defining the reference value in the third dimension. As this value remains constant and doesn't consider the variation in the geometry of the model, 2D computations provide only approximate values. Nevertheless, these computations provide enough insights into the flow physics as well as hydrodynamic forces and moments in the initial phase of any design.

Simulations have been carried out by varying the drift angle (β) from 0 to 12.5 deg in the vertical plane. The velocity contours around the UUV obtained from the simulation are presented in Figure 9. Figures from 9 (a) to 9 (f) represents different contours for various drift angles.

4.4 *Propulsion Tests*

Propulsion tests have been carried out on a 2D model through prescribed rigid body motions on the tail using the displacement function given by Equation 10

$$\phi = -\phi_a \sin(\omega t) \tag{10}$$

through the user defined functions (UDF) module of the solver.

Here ϕ is the sinusoidal tail oscillation about y-axis, ϕ_a the amplitude of motion taken here as 12.5 deg, ω is the angular frequency, 0.5 rad/s and t, the instantaneous time. The wake oscillations indicating the effective production of thrust is depicted in Figure 10.

4.5 *Dynamic manoeuvre simulations*

Hydrodynamic forces and moments are predicted here by simulating the manoeuvring motions in heave and pitch. Roll motions are not considered.

The sinusoidal motions in heave and pitch have been brought in using UDF module of the solver. The displacement functions in pitch and heave are as given by Equations 10 and 11 respectively.

$$z = z_a \sin(\omega t) \tag{11}$$

Here z_a is taken as $D/4$. Simulations have also been carried out imposing combined heave and pitch on the UUV body. Contours of total pressure around the UUV body in heave, pitch and combined motions are shown in Figures 11, 12 and 13 respectively.

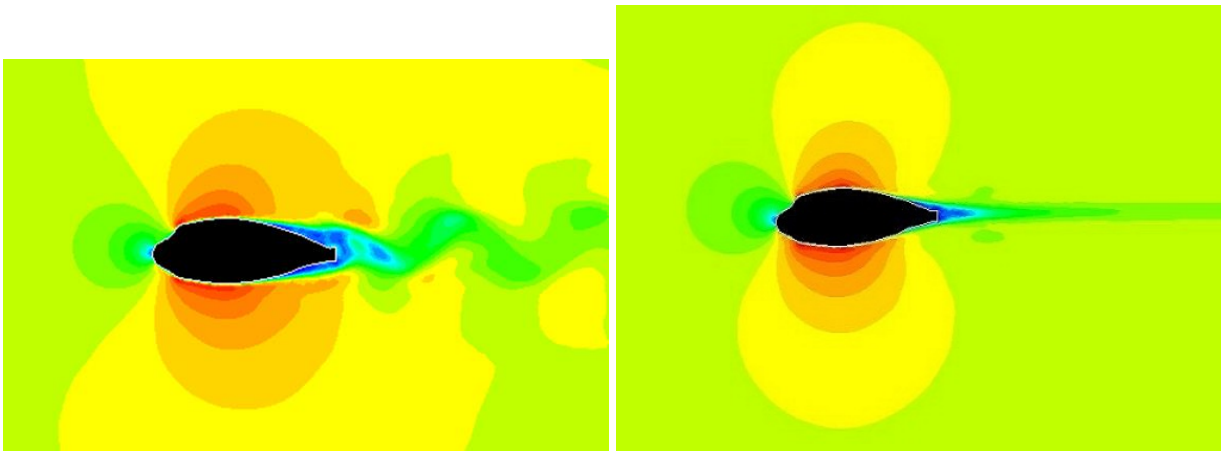

(a) 0 deg

(b) 2.5 deg

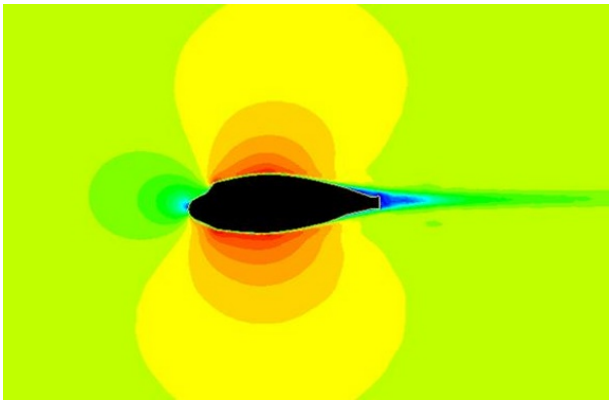

(c) 5 deg

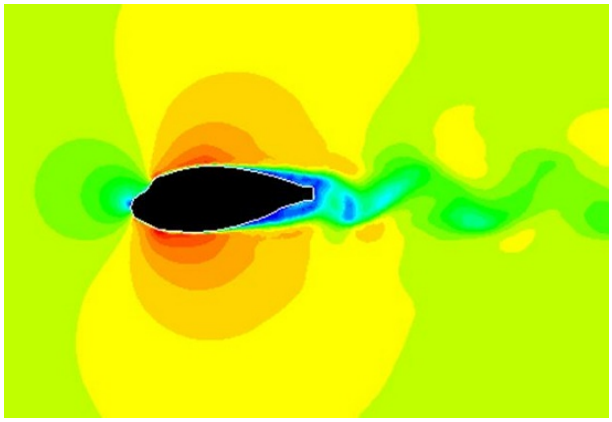

(d) 7.5 deg

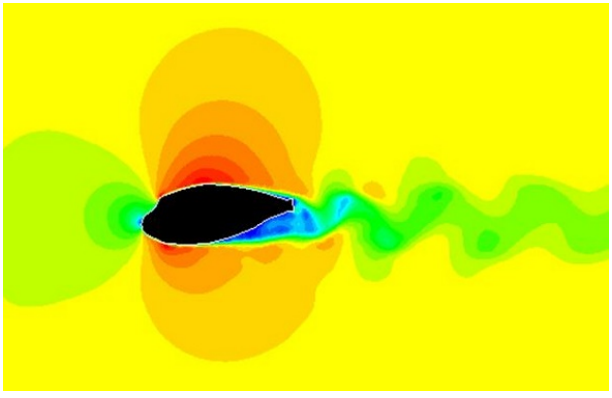

(e) 10 deg

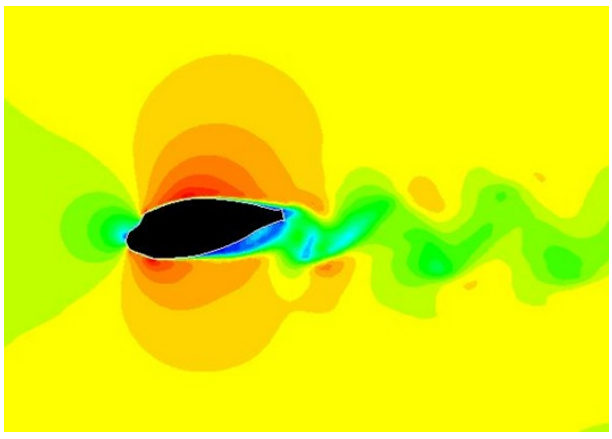

(f) 12.5 deg

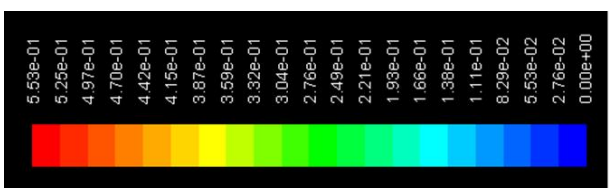

(g) Velocity Range

Figure 9: Velocity contours around the UUV at various angles of attack.

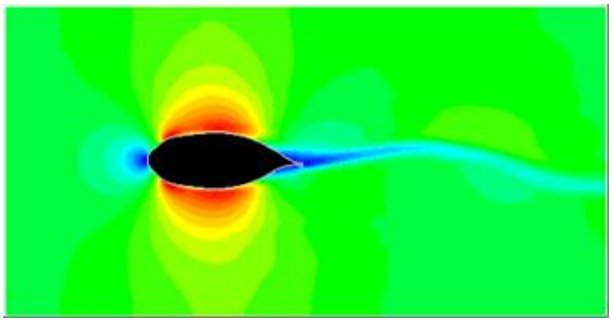

Figure 10: Wake oscillations due to tail motions

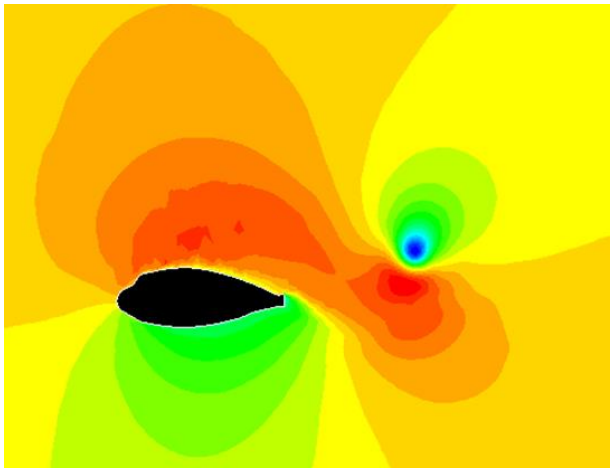

Figure 11: Total pressure contours in heave

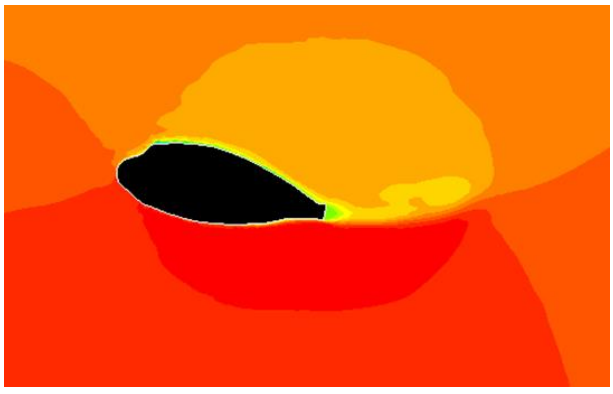

Figure 12: Total pressure contours in pitch

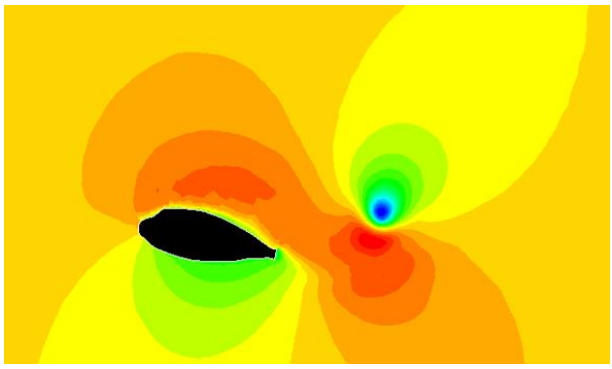

Figure 13: Total pressure contours in combined mode

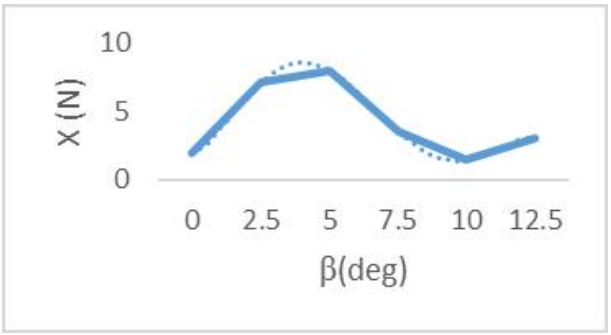

Figure 14: Variation of surge force with angle of attack

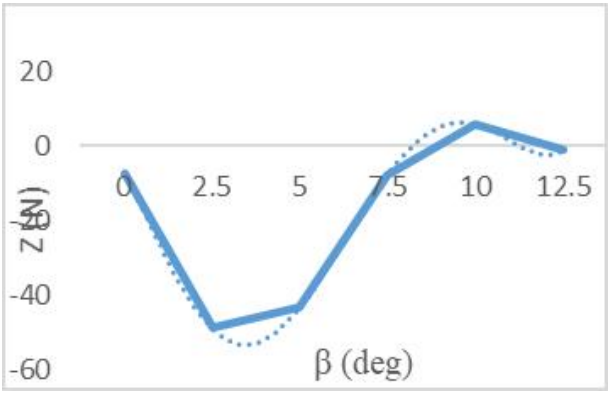

Figure 15: Variation of heave force with angle of attack

5 RESULTS AND DISCUSSIONS

In the present work manoeuvre motion simulations have been carried out on an ostraciiform locomotion inspired box-fish shaped UUV. At the outset, steady state simulations were carried out on a half model of the UUV for $Re = 0.5 \times 10^6$. The simulation yielded the value of drag coefficient, C_D as 0.019 and lift coefficient, C_L as 0.0684. The 2D simulations with an approximation of the third side yielded $C_D = 0.021$ and $C_L = 0.074$. The results show that 2D simulations can yield better results. Net surge and heave forces have been estimated using the Equations (12) and (13) respectively. As there are not much literature on this study, the results could not be verified.

$$X = F_D \cos\beta + F_L \sin\beta \tag{12}$$

$$Z = -F_D \sin\beta + F_L \cos\beta \tag{13}$$

Variation of the surge force, heave force and pitch moments with the angle of attack, β are shown in Figures 14, 15 and 16 respectively. The plots are also supplemented by a smoothing trend line.

The prediction of hydrodynamic forces and moments in the case of box-fish like bodies is not as straight forward as in the case of streamlined ships and submarines. The body being bluff, sheds vortices at moderate angles (say 7.5 deg) of attack which shows a sudden drop in surge and heave forces as well as in pitch moment. Later beyond 10 deg, the formation of vortices stabilizes and are expected to contribute to induced components of surge, heave and

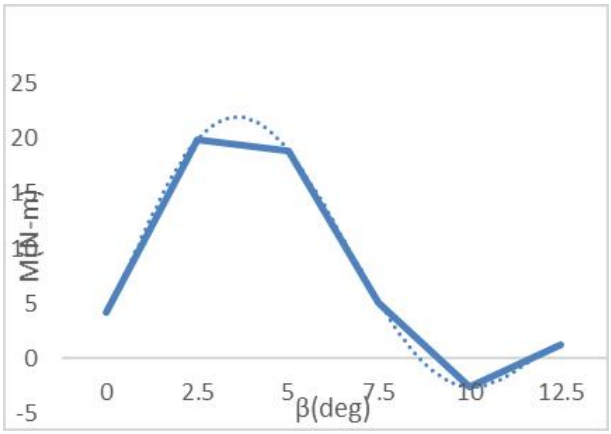

Figure 16: Variation of pitch moment with angle of attack

pitch and hence a rise in the trend is seen.The static manoeuvre simulation tests on further analysis provide the w dependent derivatives.

The propulsion simulation using the oscillation of the tail show an oscillating wake with very weak vortices shedding and disappearing in no time. Hence ostraciiform fish exhibits sluggish locomotion. The maximum thrust generated due to tail motion is found to be $X_T = 2.4N$.

Time histories of surge force, heave force and pitch moment when the UUV is subjected to pure sinusoidal heave motion is shown in Figure 17 plotted for one complete time period of oscillation ($12.56rad/s$).

Similarly, the time histories of forces and moment in pitch and combined mode is shown in Figures 18 and 19.

These plots reveal that box-fish, due to its asymmetry about y-z plane doesn't produce symmetrical surge forces while its symmetry in x-z as well as x-y planes resulted in symmetrical heave forces and pitch moments. From heave simulations, the hydrodynamic coefficients that can be evaluated are X_w, Z_w and M_w. From the pitch simulations the derivatives X_q, Z_q and M_q can be evaluated. Combined mode simulations yield coupled derivatives which are not of interest to this paper. The other derivatives can also be evaluated considering the motions in the horizontal plane and also by considering roll into account.

6 CONCLUSIONS

Box-fish owing to its non-streamlined shape has poor controllability. They need extra thrust from the pectoral fins to supplement the thrust produced by the caudal fin. Their tail length is too short to generate reverse Von-Kármán vortex street of vortices for improved power. This tail form helps the fish in sustaining power for a longer time. Nevertheless, this work provides an initial frame work for the estimation of hydrodynamic derivatives for a UUV in the form of a box fish-the simplest possible mode of implementation for bio-inspired propulsion. 2D results have helped us in reasonable qualitative predictions. Quantitatively, the results are yet to be verified either with experimental or published ones. For more accurate prediction, overset grids and 3D models are suggested.

7 FUTURE WORK

Nature has its own way of compensating for the shortcomings imposed on its own creation. The carapace on the fish's body is believed to reduce drag and direct flow such that the fish attains better manoeuvrability (Van Wassenbergh, van Manen, Marcroft, Alfaro, & Stamhuis 2015). Moreover, the role of the pectoral fins in augmenting the thrust produced by caudal fin is unexplored in the present work. The present work will be extended with the inclusion of carapace and pectoral fins in the future works. The hydrodynamic forces and moments will be analyzed using a Fourier series method (Janardhanan & Krishnankutty 2009) for obtaining the hydrodynamic derivatives of the hull form.The trajectories of the UUV in standard manoeuvres such a turning circle and zig-zag will be predicted to finally arrive at its controllability, counter-controllability and stability characteristics.

REFERENCES

Blake, R. (1977). On ostraciiform locomotion. *Journal of the Marine Biological Association of the United Kingdom 57*(4), 1047–1055.

Chandran, V., S. Janardhanan, V. Menon, et al. (2018). Numerical study on the influence of mass and stiffness ratios on the vortex induced motion of an elastically mounted cylinder for harnessing power. *Energies 11*(10), 2580.

Hinostroza, M., C. Guedes Soares, & H. Xu (2018). Motion planning, guidance and control system for autonomous surface vessel. In *ASME 2018 37th International Conference on Ocean, Offshore and Arctic Engineering*, pp. V11BT12A016–V11BT12A016. American Society of Mechanical Engineers.

Janardhanan, S. & P. Krishnankutty (2009). Prediction of ship maneuvering hydrodynamic coefficients using numerical towing tank model tests. In *12th Numerical Towing Tank Symposium*.

Schlichting, H. & K. Gersten (2016). *Boundary-layer theory*. Springer.

Van Wassenbergh, S., K. van Manen, T. A. Marcroft, M. E. Alfaro, & E. J. Stamhuis (2015). Boxfish swimming paradox resolved: forces by the flow of water around the body promote manoeuvrability. *Journal of the Royal Society Interface 12*(103), 20141146.

Wu, Z., J. Yu, Z. Su, & M. Tan (2014). Implementing 3-d high maneuvers with a novel biomimetic robotic fish. *IFAC Proceedings Volumes 47*(3), 4861–4866.

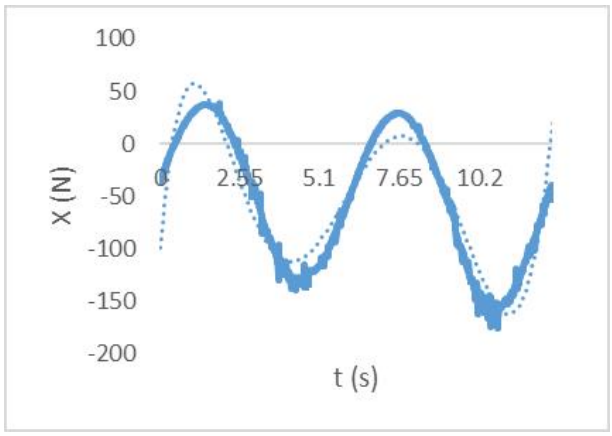

(a) Surge force

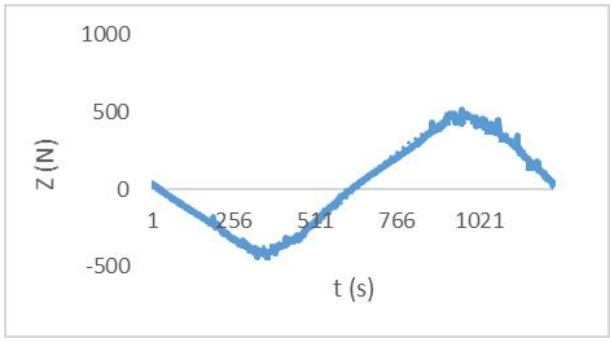

(b) Heave force

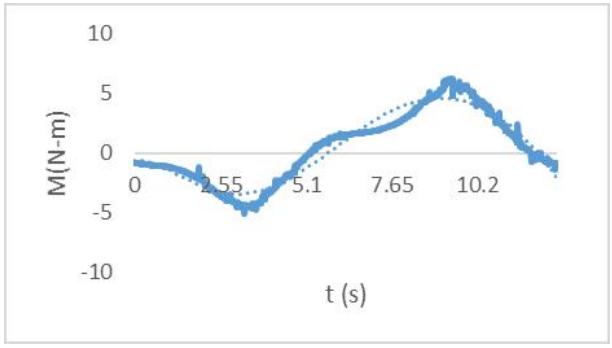

(c) Pitch moment

Figure 17: Time histories of forces and moment in heaving motion

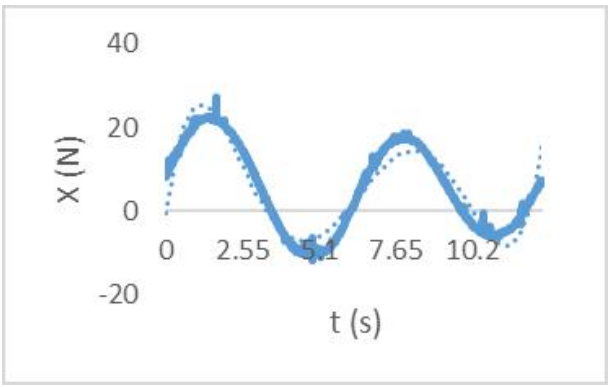

(a) Surge force

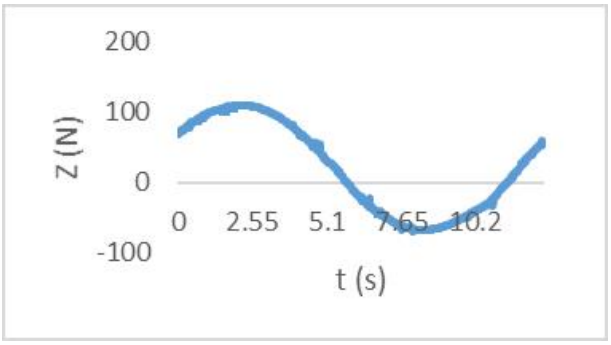

(b) Heave force

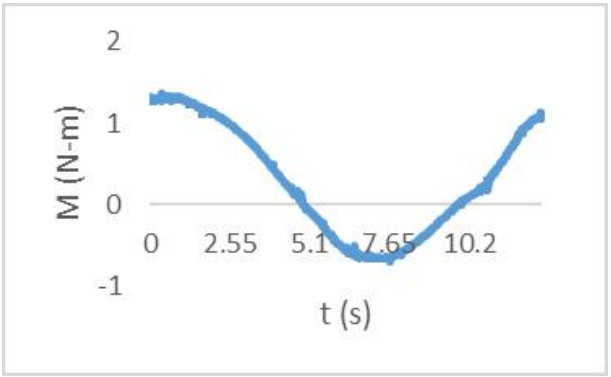

(c) Pitch moment

Figure 18: Time histories of forces and moment in pitching motion

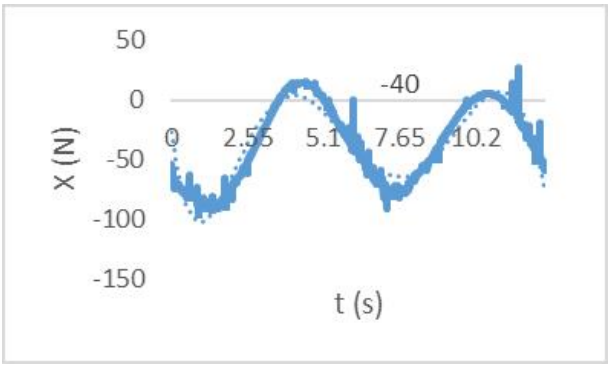

(a) Surge force

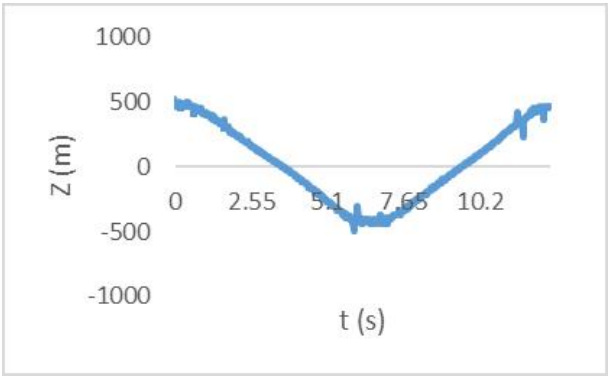

(b) Heave force

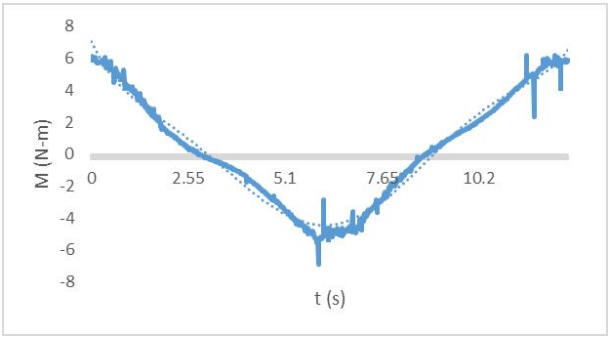

(c) Pitch moment

Figure 19: Time histories of forces and moment in surge motion

IJIREEICE

ISSN (Online) 2278-1021
ISSN (Print) 2319-5940

International Journal of Innovative Research in
Electrical, Electronics, Instrumentation and Control Engineering
NCIET- 2020
National Conference on Innovations in Engineering & Technology
Govt., Polytechnic College, Palakkad, Kerala
Vol. 8, Special Issue 1, February 2020

Evaluation of Current Design Practices for Horizontal Curves on Rural Highways Based on Vehicle Stability and Safety

Y K Remya[1], Anitha Jacob[2], E A Subaida[3]

Assistant Professor, Department of Civil Engineering, SCMS College of Engineering and Technology, Karukutty, India[1]

Lecturer, Department of Civil Engineering, Govt. Polytechnic College, Chelakkara, Thrissur, India[2]

Associate Professor, Department of Civil Engineering, Govt Engineering College, Thrissur, India[3]

Abstract: All over the world India bangs the top most position in deaths caused by road crashes. Over 1 lakh people are killed or seriously injured in road crashes in India every year, that is more than the number of people killed in all our wars put together. Sixteen children die on Indian rroads daily and there is at least one death every four minutes. Majority of the crashes are found to take place on rural highways. Rural highways are characterized by a low traffic volume and hence, speed of the vehicles is mainly controlled by the geometry. The topological conditions of India have resulted in very complex curves which include combination of horizontal curve and steep gradients up or down. In such environment, the drivers tend to choose the speeds that they perceive to be comfortable to them based on their perception of the criticality of the road geometrics ahead. Any unexpected road feature in the highway may surprise the drivers and may result in erroneous driving manoeuvres, which in turn, may end up in road crashes. As highways are meant for high speed travel, the impact of any collision that takes place will be grievous or fatal. Hence, the highways have to be designed such that their geometry directs the drivers to choose the operating speed which is in harmony with the environment.

A large number of studies are done to evaluate the effect of geometry on operating speed of rural curves. But only a few researches are done to assess the effect of geometry on the stability of vehicles. Skidding and rollover crashes are increasing dramatically, the first being more common in small vehicles like cars and the latter being more common in heavy commercial vehicles like trucks. The availability of sufficient lateral friction to counteract centrifugal force experienced by a vehicle on curve is least studied, especially in India. The values of lateral friction adopted for design of horizontal curves were developed eighty years ago by Barnett 1936; Moyer and Berry 1940. Since then, vehicle fleet has changed completely and hence the demand for lateral friction may also have changed. But the point mass equation widely used for design of horizontal curve relies on lateral friction values developed by them. Also, the equation ignores the effect of vehicular characteristics or complexity of curve geometry. So, studies focusing on revision of geometric design criteria of horizontal curves based on vehicle stability and assessment of existing margin of safety or in other words, a quantitative assessment of risk involved affecting the stability of vehicles is very important. In this paper an effort has been made to identify the gaps in current design practices and to exhibit current status of study in the field of vehicle stability on rural highways.

Keywords: Skidding, Friction, Vehicle Stability, Rollover.

I. INTRODUCTION

When a vehicle travels along a horizontal circular curve, it experiences centrifugal force outward the centre of the horizontal curve. This centrifugal force is inversely proportional to the radius of horizontal curve. Vehicle stability is achieved by the resistive forces that resist the centrifugal force. These forces include frictional interaction between the tires and pavement, and a component of the vehicle weight that acts parallel to the road surface. The frictional interaction between the tires and pavement depends on road surface side-friction factor, which in turn depends on many other factors, including road surface condition, weather and climatic condition, tire condition, and vehicle kinematics. The component of the vehicle weight that acts parallel to the road surface depends on the side slope of the highway, which is usually termed as superelevation. This approach is usually referred to as the point-mass (PM) model, which is adopted by North American design guides due to its simplicity.

Based on the point-mass model, when a vehicle travels along a vertical curve, there is obviously no centrifugal force, and consequently no potential risk for skidding or rollover. However, for 3D(combined) alignments, where a horizontal curve is superimposed by a vertical alignment, the vertical alignment affects the available side friction. For 3D alignments, traditional design guides (AASHTO 2001; TAC 1999) calculate the minimum radius assuming a side friction on a horizontal plane using the point-mass model, thus ignoring the effect of vertical alignment. This approach simplifies cornering dynamics by reducing the vehicle into a point mass travelling on a 2D horizontal alignment.

Study of the Extent of Contribution of Regional Stubble Burning to the Air Pollution in Delhi-National Capital Region

A&WMA's 112th Annual Conference & Exhibition
Québec City, Québec
June 25-28, 2019

Paper 594032

Rasma K.
PhD Student, Centre for Environmental Science and Engineering, Indian Institute of Technology Bombay, Powai, Mumbai, Maharashtra - 400076, India

Ratish Menon
Associate Professor, SCMS School of Engineering and Technology Karukutty, Ernakulam District, Kerala - 683582, India

Rakesh Kumar
Director, CSIR - National Environmental Engineering Research Institute, Nehru Marg, Nagpur, Maharashtra - 440020, India

Harish Gadhavi
Associate Professor, Space and Atmospheric Sciences Division, Physical Research Laboratory, Navrangpura, Ahmedabad, Gujarat - 380009, India

Virendra Sethi
Professor, Centre for Environmental Science and Engineering, Indian Institute of Technology Bombay, Powai, Mumbai, Maharashtra - 400076, India

ABSTRACT

The issue of extreme episodic air pollution events in the Delhi-National Capital Region (NCR), India, during the month of November has been of concern for the last few years. Recent studies have used satellite observations and transport models, which indicate movement of smoke from stubble burning regions in Punjab and Haryana towards Delhi. Quantification of contribution of these emissions to the air pollution in Delhi, however, remains uncertain. In the present study, a similar attempt was made, and measurements are reported from 16 ground-based continuous air quality monitoring stations (CAAQMS) in the Delhi-NCR for the years 2016 and 2017. Time series $PM_{2.5}$ ground measurements were compared with the total Fire Radiative Power (FRP) from Moderate Resolution Imaging Spectroradiometer (MODIS) onboard Terra and Aqua satellites for the airshed for Delhi-NCR. To quantify the smoke contribution from the fire pixels to the Delhi-NCR, the Navy Aerosol Analysis Prediction System (NAAPS) smoke data were used. NAAPS simulations show that the smoke aerosol contribution to Delhi-NCR from stubble burning was ~5-10 $\mu g/m^3$ during the pollution episodic days in 2016. NAAPS results along with the $PM_{2.5}$ measurements at Ludhiana, Punjab, indicate that the stubble burning emissions may contribute 33-66 $\mu g/m^3$ to the $PM_{2.5}$ at Delhi depending on wind conditions and emission levels at the source. The predominant aerosols over the study area during the episodic period were verified to be

Monitoring and Analysis of Gas Emissions from a Closed Landfill Site at Jleeb in Kuwait

A&WMA's 112th Annual Conference & Exhibition
Québec City, Québec
June 25-28, 2019

Paper # 601336

Ratish Menon

SCMS Water Institute, SCMS School of Engineering and Technology, Kochi, India-683582

Mohammad AlAhmad, Marwan AlDimashki

eMISK, Environment Public Authority, P. O. Box 24395 - Safat - Kuwait 13104

Vahidudeen Shanavas

Kerala State Pollution Control Board, Kadavanthara, Gandhi Nagar, Elamkulam, India- 682020

ABSTRACT

Lack of monitoring for landfill gas (LFG) emissions increases the hazard risk especially when a landfill site is being developed for further uses. This paper discusses the results from a LFG monitoring study carried out at a closed landfill site in Kuwait which lack engineered gas collection and venting system. Jleeb Al Shuyoukh landfill site was active between 1970 and 1993. The composition and seasonal variations in LFG release were monitored at Jleeb landfill site using Gasclam for the continuous LFG monitoring at 4 boreholes during the period July 2018 – Feb 2019. The monitored gases included methane (CH_4), carbon dioxide (CO_2), Carbon Monoxide (CO), Volatile Organic Compounds (VOCs), Hydrogen Sulphide (H_2S) and Oxygen (O_2). The concentration of these gases in %v/v was monitored at 1 hour interval for the entire study period along with atmospheric pressure, borehole pressure and temperature. Consistent methane release with a concentration of 40- 65 %v/v was observed at the boreholes constructed for this study. Among the monitored gases only CO_2 showed a positive correlation with methane. A constant CH_4/CO_2 ratio and lack of correlation with H_2S indicated that the landfill is in stable phase. Lack of correlation between methane release and the bore hole pressure as well as ambient temperature